frontiers | Frontiers in Immunology

TYPE Original Research
PUBLISHED 08 December 2022
DOI 10.3389/fimmu.2022.1041070

OPEN ACCESS

EDITED BY
Sergey Ponomarev,
Institute of Biomedical Problems (RAS), Russia

REVIEWED BY
Jiajia Song,
Southwest University, China
Zhigang Song,
Shandong Agricultural University, China

*CORRESPONDENCE
Yinghua Shi
annysyh@henau.edu.cn

†These authors have contributed equally to this work and share first authorship

SPECIALTY SECTION
This article was submitted to Nutritional Immunology, a section of the journal Frontiers in Immunology

RECEIVED 10 September 2022
ACCEPTED 21 November 2022
PUBLISHED 08 December 2022

CITATION
Ali Q, Ma S, Farooq U, Niu J, Li F, Li D, Wang Z, Sun H, Cui Y and Shi Y (2022) Pasture intake protects against commercial diet-induced lipopolysaccharide production facilitated by gut microbiota through activating intestinal alkaline phosphatase enzyme in meat geese. *Front. Immunol.* 13:1041070. doi: 10.3389/fimmu.2022.1041070

Pasture intake protects against commercial diet-induced lipopolysaccharide production facilitated by gut microbiota through activating intestinal alkaline phosphatase enzyme in meat geese

Qasim Ali[1†], Sen Ma[1,2,3†], Umar Farooq[4], Jiakuan Niu[1], Fen Li[1], Defeng Li[1,2,3], Zhichang Wang[1,2,3], Hao Sun[1,2,3], Yalei Cui[1,2,3] and Yinghua Shi[1,2,3*]

[1]Department of Animal Nutrition and Feed Science, College of Animal Science and Technology, Henan Agricultural University, Zhengzhou, Henan, China, [2]Henan Key Laboratory of Innovation and Utilization of Grassland Resources, Henan Agricultural University, Zhengzhou, Henan, China, [3]Henan Herbage Engineering Technology Research Center, Henan Agricultural University, Zhengzhou, Henan, China, [4]Department of Poultry Science, University of Agriculture Faisalabad, Toba Tek Singh, Pakistan

Introduction: Diet strongly affects gut microbiota composition, and gut bacteria can influence the intestinal barrier functions and systemic inflammation through metabolic endotoxemia. In-house feeding system (IHF, a low dietary fiber source) may cause altered cecal microbiota composition and inflammatory responses in meat geese via increased endotoxemia (lipopolysaccharides) with reduced intestinal alkaline phosphatase (ALP) production. The effects of artificial pasture grazing system (AGF, a high dietary fiber source) on modulating gut microbiota architecture and gut barrier functions have not been investigated in meat geese. Therefore, this study aimed to investigate whether intestinal ALP could play a critical role in attenuating reactive oxygen species (ROS) generation and ROS facilitating NF-κB pathway-induced systemic inflammation in meat geese.

Methods: The impacts of IHF and AGF systems on gut microbial composition via 16 sRNA sequencing were assessed in meat geese. The host markers analysis through protein expression of serum and cecal tissues, hematoxylin and eosin (H&E) staining, localization of NF-κB and Nrf2 by immunofluorescence analysis, western blotting analysis of ALP, and quantitative PCR of cecal tissues was evaluated.

Results and Discussion: In the gut microbiota analysis, meat geese supplemented with pasture showed a significant increase in commensal microbial richness and diversity compared to IHF meat geese demonstrating the antimicrobial, antioxidant, and anti-inflammatory ability of the AGF system.

10.3389/fimmu.2022.1041070

A significant increase in intestinal ALP-induced Nrf2 signaling pathway was confirmed representing LPS dephosphorylation mediated TLR4/MyD88 induced ROS reduction mechanisms in AGF meat geese. Further, the correlation analysis of top 44 host markers with gut microbiota showed that artificial pasture intake protected gut barrier functions via reducing ROS-mediated NF-κB pathway-induced gut permeability, systemic inflammation, and aging phenotypes. In conclusion, the intestinal ALP functions to regulate gut microbial homeostasis and barrier function appear to inhibit pro-inflammatory cytokines by reducing LPS-induced ROS production in AGF meat geese. The AGF system may represent a novel therapy to counteract the chronic inflammatory state leading to low dietary fiber-related diseases in animals.

KEYWORDS

pasture grazing, gut microbiota, intestinal alkaline phosphatase, lipopolysaccharides, oxidative stress, inflammation, Keap1-Nrf2, meat geese

Introduction

Intestinal homeostasis seems to be a defining factor for poultry health that is affected by oxidative stress either produced by heat stress or feed stress (1). The poultry birds such as broilers, layers, geese, and turkeys are continuously exposed to lipopolysaccharides (LPS) *via* different routes such as feed, water, and fine dust particles in the house that always contain some amounts of LPS. However, the major natural source of LPS is the complex community of gram-negative bacteria in the intestines (2). LPS is an outer membrane component of gram-negative bacteria such as *Enterobacteriaceae* (3), *Escherichia coli* (*E. coli*) (4), *Bacterodales* (5), and *Cyanobacteria* (6) that are recognized by toll-like receptors (TLRs), particularly TLR4 and then invade the intestinal tissues and get access to the bloodstream thereby provoking reactive oxygen species (ROS)-induced systemic diseases. This leads to a leaky gut (7) that causes diarrhea, decreased nutrient absorption, and internal fluid loss in broilers (8).

From different studies, two supporting shreds of evidence suggest that nuclear factor kappa B (NF-κB) is activated either by ROS (9) or LPS (10). Further, LPS and ROS phosphorylate NF-κB inhibitor α (*IκB-α*) and let the NF-κB migrate to the nucleus and then exert their inflammatory and apoptotic impacts by activating NF-κB pathway (11). When NF-κB pathway is established, then it consistently contributes to inducing chronic low-grade inflammation (12) through upregulating oxidative stress (N. 13), pro-inflammatory mediators i.e. inducible nitric oxide (*iNOS*) and cyclooxygenase (*COX*)-2 and pro-inflammatory cytokines (i.e. *IL-1β*, *IL-6*, and *TNF-α*) (14, 15).

Gut microbial-induced LPS-mediated NF-κB activity orchestrates chronic low-grade inflammation that is a major disease risk factor in today's animals' life (16). Thus, modifiable factors that can reduce LPS-induced inflammation may potentially modulate disease risk. Different possible modifiable factors such as feed antibiotics (17), dietary fiber and threonine (18), pectin (19), Schisandra A (12), phytochemicals (20), and oral alkaline phosphatase (21) have been used in animals to detoxify LPS. Feed antibiotics increase food-born pathogenic bacterial-induced LPS resistance (22) while phytochemicals used as anticancer drugs show minimum side effects in animals (20). Albeit different dietary fibers detoxify LPS-induced chronic low-grade inflammation (18), nobody did clearly explain the mechanisms of how dietary fibers ameliorate LPS-mediated systemic inflammation facilitated by gut microbiota in meat geese.

Different dietary fiber sources such as glucomannan, oligosaccharides, sialyl lactose, and galactooligosaccharides shape the gut microbiota to regulate intestinal ALP in rats and other animals (23, 24). Intestinal ALP is an endogenous antimicrobial peptide that is secreted from the apical enterocytes of small intestine and then moves toward the large intestine (25). Intestinal ALP has been shown to dephosphorylate LPS, CpG-DNA, and flagellin (26). In previous studies, lipid A moiety plays a role of bridge in activating myeloid differentiation factor 88 (MyD88) pathway by binding LPS with TLR4 and then activating oxidative stress (27) and NF-κB-induced systemic inflammation (12). In previous studies is not defined clearly to what extent and in which way the intestinal ALP dephosphorylates LPS by breaking TLR4/MyD88-induced ROS production and NF-κB-induced systemic inflammation. Furthermore, intestinal ALP promotes healthy homeostasis of gut microbiota (28) and gut barrier

functions (29), which has been associated with lowering systemic inflammation in several studies of healthy adults (30) and their specific health conditions (e.g. obesity, diabetes, and cardiovascular disease) (31). The increasing evidence of the salutary functions of ALP emphasizes the significance of the naturally occurring brush border enzyme. Therefore, there is a need to find optional nutritional strategies that could naturally induce and regulate the endogenous growth of intestinal ALP in poultry birds. One of the optional possible nutritional strategies is the application of dietary fiber which has been used in different studies to induce intestinal ALP production (24).

Geese are herbivorous, and because of their unique ability to use high fiber feeds, pasture was suggested to be included to promote health (32). In China, the most commonly available pasture is ryegrass, which is rich in protein, dietary fiber, fatty acids, iron, zinc, magnesium, calcium, vitamins, essential amino acids, alkaloids, steroids, flavonoids, glycosides, phenols, and tannins (33). Recently, several reports suggest that ryegrass could regulate intestinal microflora of Beijing-you chickens (34) and improve ethnomedical properties like being antioxidant, antimicrobial, and anti-inflammatory diseases in animals (35, 36). However, up to now, formal mediation analysis experiments about the association between ryegrass (high dietary fiber) intake-induced endogenous ALP-regulated kelch-like ECH-Associating protein 1-nuclear factor erythroid 2 (Keap1-Nrf2) pathway and LPS-induced oxidative stress is lacking. Moreover, the Keap1-Nrf2 system plays a central role in the regulation of the oxidative stress response, and that Nrf2 coordinately regulates cytoprotective genes (37). Here we reported that the regulation of gut microbial-induced endogenous intestinal ALP by pasture intake preserves the normal homeostasis of gut microbiota, dephosphorylates LPS/TLR4/MyD88 pathway-mediated ROS insults, and activates Keap1-Nrf2 pathway to alleviate NF-κB-induced systemic inflammation in meat geese.

Materials and methods

Ethical approval

According to animal care guidelines, the study was conducted using Wanfu geese. All used procedures were approved by the Research Bioethics Committee of the Henan Agricultural University (approval HENAU-2021).

Animals, diets, and housing

A total of 180, 25-day-old Wanfu mixed-sex geese from the commercial geese farm were purchased from Henan Daidai goose Agriculture and Animal husbandry development Co., Ltd (Zhumadian, China). The geese with an average weight of 693.6 g (± 3.32) were divided into two homogeneous groups: (1) in-house feeding group (IHF, n = 90) and (2) artificial pasture grazing group (AGF, n = 90), 12h artificial pasture grazing (06:00-18:00h) with once a day (19:00h) in-house feeding group. Each group consisted of six replicates with 15 geese per replicate. All the geese had free access to feed and freshwater *ad-libitum*. The IHF group meat geese were fed a commercial diet (Table 1). Two diets were used: a grower diet (25 to 45 days) and a finisher diet (46 to 90 days). The AGF system was established in form of grazing of meat geese at the expense of ryegrass. The nutritional composition of ryegrass was dry matter (90%), crude protein (15.47%), ash (8%), neutral detergent fiber (65%), acid detergent fiber (38%), ether extract (3.3%), calcium (0.90%), and phosphorous (0.47%). The experiment lasted for 66 days (Supplementary Figure 1).

Sample collection

Body weight and feed intake were measured every week. The pasture feed intake was measured using the method described by Cartoni Mancinelli et al. (38). On days 45, 60, and 90, we selected six healthy meat geese per replicate with a body weight range of ± 1 std. from mean 1.63-2.31 kg, 3.33-4.28 kg, and 4.38-5.39 kg respectively. Blood samples were collected in non-anticoagulant sterile blood vessels from the jugular vein. Serum samples were then obtained by centrifuging the blood samples at 4,000 × g for

TABLE 1 Nutritional composition of the diet.

	Diets	
Ingredients, %	**Grower**	**Finisher**
Wheat	57.3	59
Rice bran	5	4
Corn germ cake (exp.)	4	3.2
Corn oil	5	7
Dumpling powder	3	2
Corn distiller's grains (DDGS)	6.5	7
Spouting germ meal	3	2
Soybean meal (sol.)	7	6
Peanut meal (sol.)	1.5	1
Albumen powder	2	1.5
Stone powder	1.1	1
Liquid methionine	0.25	0.3
MuLaoDa-2	1.25	2
201/202 gunk	2.5	3
Calcium hydrogen phosphate	0.6	1
Chemical composition (%)		
Crude protein	20.12	15.54
Ash	12.89	12.86
Neutral detergent fiber	13.25	30.55
Acid detergent fiber	5.5	27.02
Calcium	1.15	1.07
Phosphorous	0.47	0.32

15 minutes at 4°C and stored at –80°C until analysis. After blood sampling, the geese were slaughtered and pH was determined from the proventriculus, gizzard, ileum, and cecum. Fresh cecal chyme was collected from the cecum using sterile 5 ml centrifuge tubes and then stored at –80°C for further analysis. The cecal tissues were immediately removed, thoroughly washed with phosphate-buffered saline (PBS), stored in liquid nitrogen, and then preserved at –80°C for further analysis. Cecal tissues were fixed by immersion in 4% and 10% neutral buffered formalin.

Measurement of LPS, ROS, and ALP levels

The serum and cecal tissues were sampled to measure LPS, ROS, and ALP activities. The kits were purchased from Shanghai Enzyme Link Biotechnology Co., Ltd (Shanghai, China) and all experimental procedures were performed according to the manufacturer's instructions.

Bacterial growth conditions

LPS is a key virulence factor of Escherichia coli (E. coli) that triggers innate immune responses *via* activation of the toll-like receptor 4 signaling pathway (39). To identify, whether *E. coli* contributes to activating the LPS, the batch cultivation for *E. coli* was carried out in Luria broth (LB) medium at 37°C with a 2-L working volume. LB medium was from recipe of Miller (5 g yeast extract, 10 g peptone tryptone, 10 g NaCl) (40). The pH was maintained at 6.95 automatically by titration with 5% H_2SO_4 or 5% NaOH. Ampicillin was added to control the growth of other bacteria. Peptone tryptone and yeast extract were from OXOID, NaCl from Sigma, agar, and ampicillin from Solarbio (life sciences). The medium was made in distilled water and autoclaved under standard conditions. Dissolved oxygen in the culture was maintained at 40% saturation automatically by varying the speed of impeller rotation. Culture growth (OD600) was monitored with a DU640 Spectrophotometer (Beckman). Further, *E. coli* was cultured onto the Petri dishes for 24h at 37°C. The CFU/g stool for *E. coli* from the Petri dishes was counted.

Measurement of gut permeability

The concentration of tight junction proteins is a widely recognized indicator known as gut permeability. For this, the tight junction proteins ZO-1, Occludin, and Claudin concentrations were determined from the cecal tissues in the present study. The kits were purchased from Shanghai Enzyme Link Biotechnology Co., Ltd (Shanghai, China) and all experimental procedures were performed according to the manufacturer's instructions. Further, mRNA expression levels of *ZO-1*, *Occludin*, and *Claudin* and 2 genes encoding tight junction proteins *dlg1* and *E-cadherin* were also measured from cecal tissues for gut barrier functions. Details related to gene expression are proposed to be harmonized in section 2.14.

Measurement of antioxidant parameters

Heme oxygenase 1 (HO-1) and glutathione reductase (GSR) were measured from serum using ELISA kits (Shanghai Meilian Biology Technology, Shanghai, China). The total superoxide dismutase (T-SOD, #A001-1), glutathione peroxidase (GSH-Px, #A005), total antioxidant capacity (T-AOC, #A015-2–1), malondialdehyde (MDA, #A003-1), and catalase (CAT, #A007-1) were measured using diagnostic kits (Nanjing Jiancheng Bioengineering Institute, Nanjing, Jiangsu, P. R. China) according to the manufacturer's instructions.

Measurement of metabolic (plasma lipid) profiles

Serum total cholesterol (T-CHO, #A111-1-1), low-density lipoprotein cholesterol (LDL-C, #A113-1-1), high-density lipoprotein cholesterol (HDL-C, #A112-1-1), triglycerides (TG, #A110-1-1), and blood urea nitrogen (BUN, #C013-1-1) was enzymatically determined using a kit from Nanjing Jiancheng Bioengineering (Nanjing, Jiangsu, P. R. China) following the manufacturer's instructions. Fasting blood glucose level was determined by a blood glucose meter (www.sinocare.com).

Hematoxylin and eosin staining

First, the cecal tissues were fixed with 10% paraformaldehyde and stained with Harris' hematoxylin solution for 6h at a temperature of 60-70°C and were then rinsed in tap water until the water was colorless. Next, 10% acetic acid and 85% ethanol in water were used to distinguish the tissue 2 times for 2h and 10h, and again the tissues were rinsed with tap water. In the bluing step, we soaked the tissue in saturated lithium carbonate solution for 12h and then rinsed it with tap water. Finally, staining was achieved with eosin Y ethanol solution for 48h.

Paraffin embedding

The tissues were dehydrated with 95% ethanol twice for 0.5h, and then soaked in xylene for 1h at 60-70°C followed by paraffin for 12h. For the cecal tissues, we used 0.5 ml of 95% ethanol in dehydration.

Slicing and imaging

The stained tissues were cut into 3 sections of 7-μm slices with well-oriented parts using a Leica RM2235 microtome and then imaged using Nikon NIS-Elements microscopy.

Localization of NF-κB and Nrf2 by immunofluorescence analysis

The tissue sections were fixed in 4% paraformaldehyde for 10 minutes. Paraffin sections were dewaxed with xylene for 15 minutes, dehydrated with gradient alcohol, and rinsed in distilled water. Dewaxed and rehydrated slides of cecal tissue sections were boiled in citrate-EDTA antigen retrieval solution for 2 minutes and were blocked with 10% fetal bovine serum for 30 minutes. The tissue sections were incubated for NF-κB and Nrf2 with primary antibody Rabbit Anti-NF-κB (Affinity, P65-AF5006, 1:200; v/v) or Rabbit anti-Nrf2 (Bioss, bs-1074R, 1:500; v/v) respectively, at 4°C overnight followed by secondary antibody (HRP Goat Anti-Rabbit IgG (SeraCare, 5220-0336, 1:400; v/v) with incubation at room temperature in the dark for 50 minutes. Tyramine salt fluorescein was added dropwise to the tissues (configured with phosphate-buffered saline with Tween 20 (PBST) containing 0.0003% H_2O_2) and incubated at room temperature for 20 minutes. 4',6-dia-midino-2-phenylindole (DAPI) was used to incubate the slides for 10 minutes at room temperature. Finally, the slides were sealed with anti-fluorescent quenching mounting medium, and the localization of Nrf2 and NF-κB was detected with a confocal fluorescence microscope (TCSSP8STED, Leica, Wetzlar, Germany). The nuclei stained by DAPI are blue under ultraviolet excitation and are positively expressed as the corresponding fluorescein-labeled green light.

Western blotting analysis of ALP

The cecal tissues were harvested and cut open longitudinally, and luminal contents were removed. The tissues were washed with phosphate-buffered saline (PBS) and homogenized with liquid nitrogen, and homogenates were mixed with radioimmunoprecipitation assay (RIPA) buffer (50 mM Tris-HCl, pH 7.4, 150 mM NaCl, 1% Triton X-100, 1% sodium deoxycholate, 0.1% sodium dodecyl sulfate) containing protease inhibitor cocktail (Sigma Aldrich), incubated on ice for 30 minutes, and centrifuged at 12,000 rpm for 5 minutes at 4°C. Proteins (50 ng/sample) were solubilized and heating denaturation in 40 mL of sodium dodecyl sulfate (SDS) loading buffer (SolarBio, Shanghai, China) and then resolved by electrophoresis (BioRad, Hercules, CA, USA) on 10% SDS-PAGE gels prior to electrophoretic transfer to polyvinylidene fluoride (PVDF) membranes (Millipore, Billerica, MA, USA). Standard markers for protein molecular masses were purchased from Thermo (Waltham, MA, USA). The membranes were blocked with 5% nonfat dry milk (NFDM) in Tris-buffered saline with 0.05% Tween 20 (TBS-T, Solarbio, Shanghai, China) for 1h at room temperature and then probed with 1:1,000 dilution of rabbit ALP primary antibodies (ET1601-21, huabio, Hangzhou, China) and GAPDH primary antibodies (MAB45855, Bioswamp, Wuhan, China) in 5% BSA at 4°C overnight. After washing three times in TBS-T, the blots were further incubated with 1:3,000 dilution of a horseradish peroxidase (HRP)-conjugated goat anti-rabbit IgG antibody (E-AB-1003, Elabscience, Wuhan, China) or HRP-conjugated goat anti-rabbit IgG antibody (E-AB-1001, Elabscience, Wuhan, China) at 37°C for 1h. The proteins were visualized using Beyo ECL reagents (Beyotime, Shanghai, China). The intensity of the bands was quantified with a Pro Plus 6.0 Biological Image Analysis System.

RNA extraction and RT-qPCR

Total RNA from the cecal tissues (about 50 to 100 mg) was extracted by the addition of 1 mL of MagZol-reagent (#R4801-02; Magen Biotechnology, Guangzhou, Guangdong, China) according to the manufacturer's instructions. The concentration and purity of the total RNA were assessed using a NanoDrop 2000 UV-vis spectrophotometer (Thermo Scientific, Wilmington, USA). Subsequently, the RNA was reverse transcribed to cDNA using the ReverTra Ace® qPCR RT Master Mix with gDNA Remover (TOYOBO, OSAKA, Japan) according to the manufacturer's instructions. The cDNA samples were amplified by real-time quantitative polymerase chain reaction with ChamQ Universal SYBR qPCR Master Mix from Vazyme Biotechnology (Nanjing, Jiangsu, P. R. China). Gene-specific primers for each gene were designed using Primer3web, version 4.1.0 (Supplementary Table 1). PCR was performed on the C1000 Touch PCR Thermal cycler (BIO-RAD Laboratories, Shanghai, China) using ChamQ Universal SYBR qPCR Master Mix from Vazyme Biotechnology (Nanjing, Jiangsu, P. R. China) and was as follows: 40 cycles of 95°C for 15 s and 60°C for 30 s. All measurements will be performed in triplicate. The messenger ribonucleic acid (mRNA) expression of target genes relative to beta-actin (*β-actin*) was calculated using $2^{-\Delta\Delta CT}$ method (41).

DNA extraction and PCR amplification

According to the manufacturer's instructions, the microbial community genomic DNA was extracted from cecal chyme samples using the E.Z.N.A.® soil DNA Kit (Omega Bio-Tek, Norcross, GA, U.S.). The DNA extract was checked on 1% agarose gel, and DNA concentration and purity were determined with NanoDrop 2000 UV-vis spectrophotometer (Thermo

Scientific, Wilmington, USA). The hypervariable region V3-V4 of the bacterial 16S rRNA gene was amplified with primer pairs 338F (5'-ACTCCTACGGGAGGCAGCAG-3') and 806R (5'-GGACTACHVGGGTWTCTAAT-3') by an ABI GeneAmp® 9700 PCR thermocycler (ABI, CA, USA). The PCR amplification of the 16S rRNA gene was performed as follows: initial denaturation at 95°C for 3 minutes, followed by 27 cycles of denaturing at 95°C for 30 s, annealing at 55°C for 30 s, and extension at 72°C for 45 s, and single extension at 72°C for 10 minutes, and end at 4°C. The PCR mixtures contain 5 × *TransStart* FastPfu buffer 4 μL, 2.5 mM dNTPs 2 μL, forward primer (5 μM) 0.8 μL, reverse primer (5 μM) 0.8 μL, *TransStart* FastPfu DNA Polymerase 0.4 μL, template DNA 10 ng, and finally ddH_2O up to 20 μL. PCR reactions were performed in triplicate. The PCR product was extracted from 2% agarose gel and purified using the AxyPrep DNA Gel Extraction Kit (Axygen Biosciences, Union City, CA, USA) according to the manufacturer's instructions and quantified using Quantus™ Fluorometer (Promega, USA).

Illumina MiSeq sequencing

Purified amplicons were pooled in equimolar, and paired-end sequenced (2 ×300) on an Illumina MiSeq platform (Illumina, San Diego, USA) according to the standard protocols by Majorbio Bio-Pharm Technology Co., Ltd. (Shanghai, China).

Processing of sequencing data

The raw 16S rRNA gene sequencing reads were demultiplexed, quality-filtered by Trimmomatic, and merged by FLASH with the following criteria: (i) the 300 bp reads were truncated at any site receiving an average quality score of <20 over a 50 bp sliding window, and the truncated reads shorter than 50 bp were discarded, reads containing ambiguous characters were also discarded; (ii) only overlapping sequences longer than 10 bp were assembled according to their overlapped sequence. The maximum mismatch ratio of overlap region is 0.2. Reads that could not be assembled were discarded; (iii) samples were distinguished according to the barcode and primers, and the sequence direction was adjusted, exact barcode matching, 2 nucleotides mismatches in primer matching. The taxonomy of each OTU representative sequence was analyzed by RDP Classifier (http://rdp.cme.msu.edu/) against the 16S rRNA database (e.g. Silva SSU128) using a confidence threshold of 0.7. The species composition and relative abundance of each sample were counted at the phylum level, and the composition of the dominant species of different groups was visualized by the package pie chart of R (version 3.3.1) software. PICRUSt is a software package for the functional prediction of 16S amplicon sequencing results which was used to determine the COG IDs related to LPS production. Spearman rank correlation coefficient was performed to construct a correlation heatmap among the highly abundant GO terms and cecal microbiota at phylum as well as genus levels mostly relevant to LPS production. Further, to determine the effect of microbiota interacting with apparent performance, redundancy analysis (RDA) was performed at the genus level using the R language vegan packet on Spearman correlation analysis (RDA 2014).

Statistical analysis

Data were expressed as mean ± SEM. Statistical analyses were performed using SPSS 20.0 software (=D3 SPSS, Inc., 2009, Chicago, IL, USA www.spss.com). Data from two groups were evaluated by unpaired two-tailed student T-Test. Significance was considered to be at $P< 0.05$. Spearman correlation analysis of the Euclidean distance was performed using GraphPad Prism version 8.3.0., and origin 2021. To compare host markers' relationships, Pearson's correlation analysis was performed by OECloud tools (https://cloud.oebiotech.cn).

Results

Artificial pasture grazing system modulates gut microbiota to inhibit LPS synthesis induced by in-house feeding system

The metagenome predicted functions classified using clusters of orthologous genes (COG) database in phylogenetic reconstruction of unobserved states (PICRUSt) software are performed to investigate the functional differences in the gut microbiota between the two feeding meat geese groups (in-house feeding group (IHF) and artificial pasture grazing group (AGF) meat geese) at different time points 45d, 60d, and 90d. A total of 4060, 4069, 4082, 3959, 4030, and 4060 COG IDs were identified in samples IHF45, AGF45, IHF60, AGF60, IHF90, and AGF90 respectively (unpublished data). To identify which strains contribute to LPS production in the meat geese gut, we focused on the GO terms and cecal microbiota at the phylum level mainly relevant to LPS biosynthesis (Figure 1A and Supplementary Figures 2A–F). At 45d, in the IHF meat geese, *Firmicutes* families dominated the four while *Actinobacteiota* dominated the two main COG terms related to LPS biosynthesis. At 60d, in the IHF meat geese, *Actinobacteriota* and *Proteobacteria* families dominated the four and two main COG terms related to LPS biosynthesis, respectively. At 90d, only *Bacteroidota* family dominated the three main COG terms related to LPS biosynthesis in IHF meat geese.

Overall, *Firmicutes* and *Bacteroidota* families dominate both in the IHF and AGF meat geese at 45d, 60d, and 90d, but

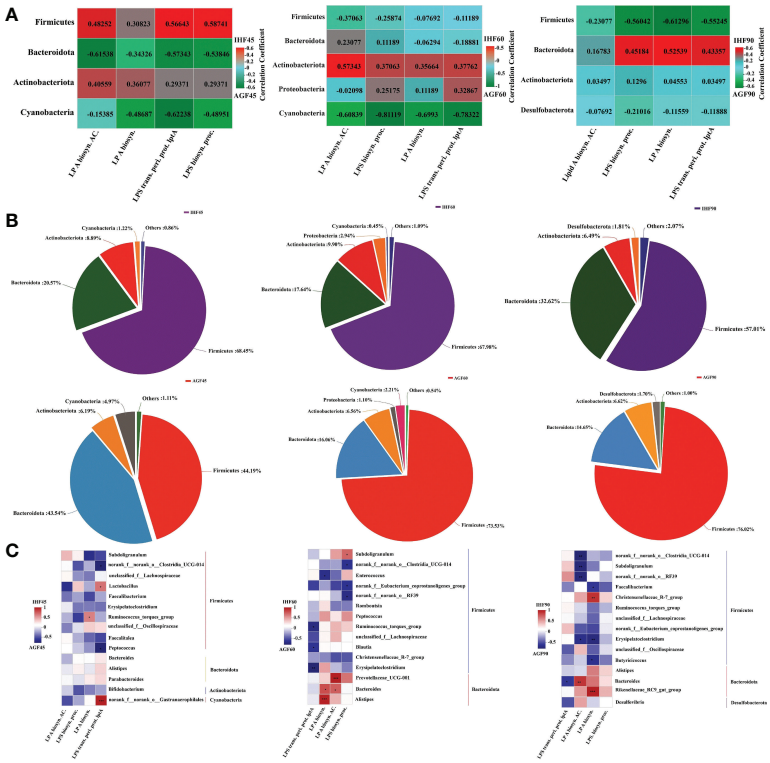

FIGURE 1
Artificial pasture grazing system modulates gut microbiota to inhibit LPS synthesis induced by in-house feeding system. **(A)** Average abundance per sample of genes related to the four main LPS biosynthesis-related functions. Red indicates a positive correlation; green indicates a negative correlation, **(B)** Relative contributions of the different phyla to the total LPS-encoding capacity of the gut microbiome, and **(C)** Contribution of individual genera to LPS biosynthesis functions. The average abundances of genes related to any of the four LPS-related GO functions are shown for individual genera within each phylum. LP A biosyn. AC.; lipid A biosynthesis acyltransferase, LP A biosyn.; lipid A biosynthesis, LPS trans. peri. prot. lptA; lipopolysaccharide transport periplasmic protein lptA, and LPS biosyn. proc.; lipopolysaccharide biosynthesis process. Red indicates a positive correlation; blue indicates a negative correlation. In-house feeding system (IHF) and artificial pasture grazing system (AGF). The asterisks symbol indicates significant differences *P < 0.05, **P < 0.01, ***P < 0.001

Firmicutes and *Bacteroidota* individually contribute 68.45% and 32.62% of the LPS biosynthesis in the IHF meat geese at 45d and 90d, respectively (Figure 1B). In contrast, *Actinobacteriota* family is the minor contributor to LPS biosynthesis, with an average of 8.89% and 9.90% of the total LPS biosynthesis in IHF meat geese at 45d and 60d, respectively. In contrast to other bacterial families, *Proteobacteria* family with a minute quantity with an average of 2.94% contributes to the total LPS biosynthesis in IHF meat geese at 60d.

The quality and types of diet make alterations in the gut microbiota in a time-dependent manner. We next examined whether the bacterial composition of the samples would correlate with the potency of activation or inhibition of these samples (Figure 1C). At the genus level, we determined the Spearman correlation between the GO terms and cecal microbiota falling in different phyla mainly relevant to LPS biosynthesis and those have been individually expressed in a supporting file (Supplementary Figures 3A–E). We identify a strong correlation between GO functions related to LPS biosynthesis and microbial composition at the genus level and could only find a moderate-to-strong correlation between a few microbial individual genera and the stimulatory potency of individual cecal LPS production in IHF meat geese (Figure 1C). However, we found that the abundance of very few bacterial genera *Lactobacillus* and *Ruminococcus_torques_group* following *Firmicutes* phylum show a moderate correlation with the activation of lipid A biosynthesis and LPS transportation periplasmic protein lptA at 45d in IHF meat geese (Figure 1C). While only single bacterial genera *norank_f:norank_o: Gastranaerophilales* following the phylum *Cyanobacteria* show a strong correlation with the activation of LPS transportation periplasmic protein lptA at 45d in IHF meat geese (Figure 1C). In contrast, we found a maximum of the bacterial genera *Prevotellaceae_UCG-001*, *Bacteroides*, and *Alistipes* following *Bacteroidota* phylum were contributing to the lipid A biosynthesis acyltransferase and lipid A biosynthesis at 60d in IHF meat geese (Figure 1C). Similarly, *Bacteroides* and *Rikenellaceae_RC9_gut_group* following *Bacteroidota* phylum

follow the same trend in activating the lipid A biosynthesis acyltransferase and lipid A biosynthesis at 90d in IHF meat geese (Figure 1C). Notably, *Bacteroides* dominate activating lipid A biosynthesis acyltransferase at 60d and 90d in IHF meat geese (Figure 1C). Our results revealed that *Bacteroidota* phylum is by far the most abundant contributor to the LPS biosynthesis functions in IHF meat geese intestinal microbiota, consistent with their high abundance relative to other Gram-negative genera in the gut.

Inhibitory effects of artificial pasture grazing system on in-house feeding system-induced ROS production *via* LPS/TLR4/MyD88 pathway in meat geese

We observed significantly increased in pH of proventriculus, gizzard, ileum, and ceca in the AGF meat geese compared with IHF meat geese (Supplementary Figures 4A–D and Supplementary Table 2). Then we measured the protein levels of intestinal ALP activity and expression levels of intestinal alkaline phosphatase gene (*ALPi*) and 2 separate alkaline phosphatase genes (*CG5150* and *CG10827*) from the meat geese. The serum ALP activity by enzyme-linked immunosorbent *assay* (ELISA) kit (Figure 2A) and mRNA expression of *ALPi* (Figure 2B) and alkaline phosphatase genes (*CG5150* and *CG10827*) (Figure 2C) increased significantly in AGF meat geese as compared to IHF meat geese at 45d, 60d, and 90d. Furthermore, intestinal ALP may contribute to maintaining the normal gut microbial homeostasis by suppressing the *E. coli* and as well as detoxifying the LPS (42, 43). To identify, whether *E. coli* contributes to activating the LPS and the suppression of intestinal ALP, we cultured the *E. coli* onto the Petri dishes for 24h at 37°C. For this, we counted the colony-forming units (CFU) for *E. coli* from the Petri dishes. We observed that the CFU/g stool was less in the AGF meat geese compared with the IHF meat geese (Supplementary Figure 5A). To further verify our results, we pick up one colony from the petri dish and incubated it in the LB medium for 48h at 37°C. Then we determined the *E. coli* cell cultures based on spectrophotometer readings at OD600 for 48h with an interval of 2h. We found a significant decline in the concentration of *E. coli* cell cultures from the AGF meat geese as compared to IHF meat geese (Supplementary Figure 5B).

The genes in rfa cluster such as *rfaK* and *rfaL* are involved in the synthesis and modification of LPS core. These two genes play a vital role in the attachment of 0 antigens to the core. This result was following the higher protein abundance of serum LPS (Figure 2D)

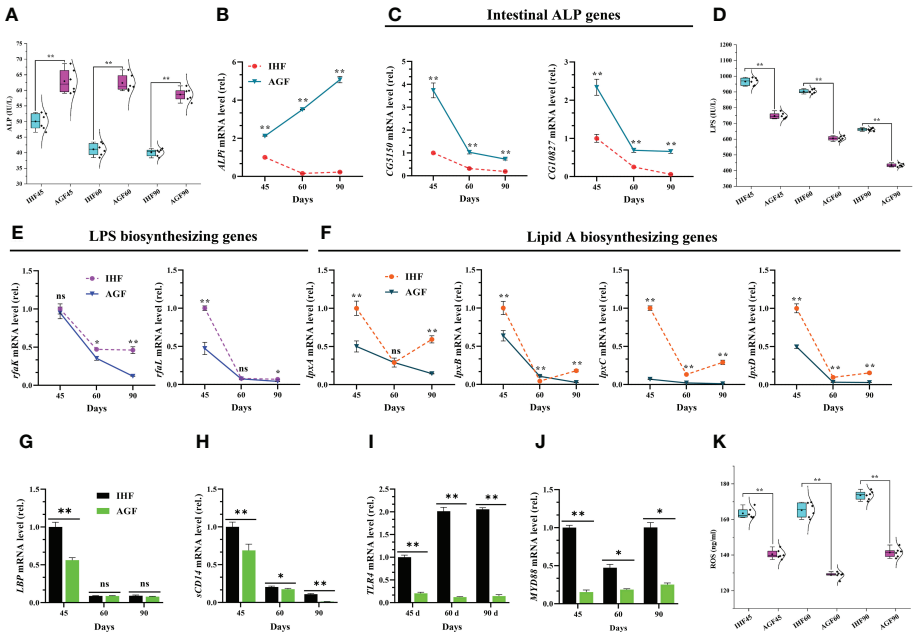

FIGURE 2
Inhibitory effects of artificial pasture grazing system on in-house feeding system-induced ROS production *via* LPS/TLR4/MyD88 pathway in meat geese. **(A)** ALP protein level in serum, **(B)** *ALPi* mRNA level in cecal tissues, **(C)** mRNA levels of intestinal ALP genes (*CG5150* and *CG10827*) in cecal tissues, **(D)** LPS protein level in serum, **(E)** mRNA levels of LPS biosynthesizing genes (*rfaK* and *rfaL*) in cecal tissues, **(F)** mRNA levels of lipid A biosynthesizing genes (*lpxA*, *lpxB*, *lpxC*, and *lpxD*) in cecal tissues, **(G)** *LBP* mRNA level in cecal tissues, **(H)** *sCD14* mRNA level in cecal tissues, **(I)** *TLR4* mRNA level in cecal tissues, **(J)** *MyD88* mRNA level in cecal tissues, and **(K)** ROS protein level in serum, normalized by *β-actin* and measured by qPCR. In-house feeding system (IHF) and artificial pasture grazing system (AGF). Data with different superscript letters are significantly different ($P < 0.05$) according to the unpaired student T-Test. The asterisks symbol indicates significant differences $^*P < 0.05$, $^{**}P < 0.01$.

and mRNA expression of LPS biosynthesizing genes *rfaK* and *rfaL* (Figure 2E) in cecal tissues of IHF meat geese. Next, to identify whether lipid A moiety of LPS permits LPS to bind with TLR4 and then activate MyD88 pathway, first, we determined the genes related to lipid A biosynthesis. We found that the mRNA expression of *lpxA*, *lpxB*, *lpxC*, and *lpxD* was lesser in the AGF meat geese compared with IHF meat geese (Figure 2F). Next, we found decreased mRNA expression of *LBP* (Figure 2G) and *soluble cluster of differentiation 14* (*sCD14*) (Figure 2H) in AGF meat geese. This suggests that the higher mRNA expression of genes related to lipid A may able the LPS to attach with *TLR4* (Figure 2I) and then activate MyD88 dependent pathway in cecal tissues of IHF meat geese compared with AGF meat geese at 45d, 60d, and 90d (Figure 2J). The activation of TLR4/MyD88 pathway may contribute to ROS production (44). As expectedly, the higher *TLR4/MyD88* gene expression was observed to be increased in IHF meat geese concerning higher serum ROS production (Figure 2K).

Inhibitory effects of artificial pasture grazing system on in-house feeding system deteriorated nutrient absorption

In our study, we found that intestinal ALP activity (Majorbio i-Sanger cloud platform (http://rdp.cme.msu.edu/)) was decreased in IHF meat geese along with increased ROS abundances (Figure 2K) compared with AGF meat geese. Based on this scenario, next, to identify whether the IHF-induced intestinal dysbiosis may impact intestinal morphology in meat geese, we performed H&E staining of cecal tissues. The effect of AGF system on the morphology of cecal tissues is presented in Supplementary Table 3. Irrespective of a commercial diet, the villus height, villus width, surface area, and distance between villi in cecum of AGF meat geese group were improved as opposed to crypt depth compared to those of IHF meat geese group at different time points 45d, 60d, and 90d. While the villus height to crypt depth ratio (V:C) values of the cecum were not different. Further, the morphology of the cecal tissues from different feeding systems was measured and compared to one another as shown in Supplementary Figure 6. These results illustrated the nutrient absorption in cecum under different feeding systems.

Beneficial effects of artificial pasture grazing system on in-house feeding system-dependent apoptosis-induced gut permeability in meat geese

Alterations in mitochondrial membrane permeability could initiate the stimulation of cytochrome C into the cytoplasm, which activates caspases that, in turn, trigger apoptosis. Before starting apoptosis-related experiments, we confirmed that cytochrome C activity was increased with a commercial diet in the cecal tissues of IHF meat geese (Majorbio i-Sanger cloud platform (http://rdp.cme.msu.edu/)), then further we confirmed it from the mRNA expression of *cytochrome C* from cecal tissues (Figure 3A). To discover that apoptosis production is affected by feed type in meat geese, we tested mRNA expression levels of *caspase 3* and *8* in cecal tissues from IHF and AGF meat geese at different stages such as 45d, 60d, and 90d. We found a significant increase in *caspase3* (*CASP3*) and *8* (*CASP8*) activity in IHF meat geese (Figures 3B, C). Next, we performed H&E staining of cecal tissues. The upper normal limit for the number of apoptotic cells per field (Mean ± SD) in the villus at 45d, 60d, and 90d from the cecal tissues of IHF and AGF meat geese has been shown in Figure 3D and Supplementary Table 4. From different studies, this accelerated apoptosis has been involved in inducing intestinal mucosa disruption and intestinal permeability (45). To evaluate whether the mucus phenotype can be explained by altered structural organization of the mucosal barrier, we stained cecal tissues with H&E. A well-defined mucus-producing goblet cell genes (mucin2 (*MUC2*) and Mucin 5, subtype AC (*MUC5AC*)), the number of goblet cells per 20μm, and inner muscular tonic/muscularis mucosa layer thickness were observed in AGF meat geese group (Figures 3E, F; Supplementary Figures 7A; 8A, B and Supplementary Table 5). In agreement with a mucosal barrier, the mucus-producing goblet cell genes and inner muscular tonic/muscularis mucosa layer appeared less organized upon a commercial diet feeding. Furthermore, intestinal ALP is known to promote gut barrier function, and the disruption of the intestinal barrier is thought to play a critical role in gut permeability development, hence, we measured the gut permeability in IHF and AGF meat geese at 45d, 60d, and 90d. The ELISA kit method showed an IHF-dependent increase in endotoxemia (LPS) (Figure 2D), significantly influenced by intestinal ALP deficiency in IHF meat geese (previously explained in Figures 2A–C). Furthermore, expression levels of intestinal tight junction proteins were measured in cecal tissues of IHF and AGF meat geese. Again diet and loss of endogenous ALP were associated with a significant reduction in protein expression levels of zona occludin-1 (ZO-1), Occludin, and Claudin (Figures 3G–I).

Inhibitory Effects of artificial pasture grazing system on in-house feeding system-induced NF-κB pathway and its systemic inflammation

In our study first, we explained that the activation of MyD88 dependent pathway could lead to the stimulation of ROS in IHF meat geese. Along with this dependent pathway, the cellular protein LC8 (8-kDa dynein light chain) plays a role in the redox regulation of NF-κB pathway. Actually, LC8 binds to *IkB-a* in a redox-dependent manner, thereby preventing its phosphorylation by IKK (46). Here, IHF system-induced intestinal ALP disruption and the resulting ROS production oxidized LC8 which leads to the dissociation from *IkB-a* and then causes *NF-κB* activation. This

10.3389/fimmu.2022.1041070

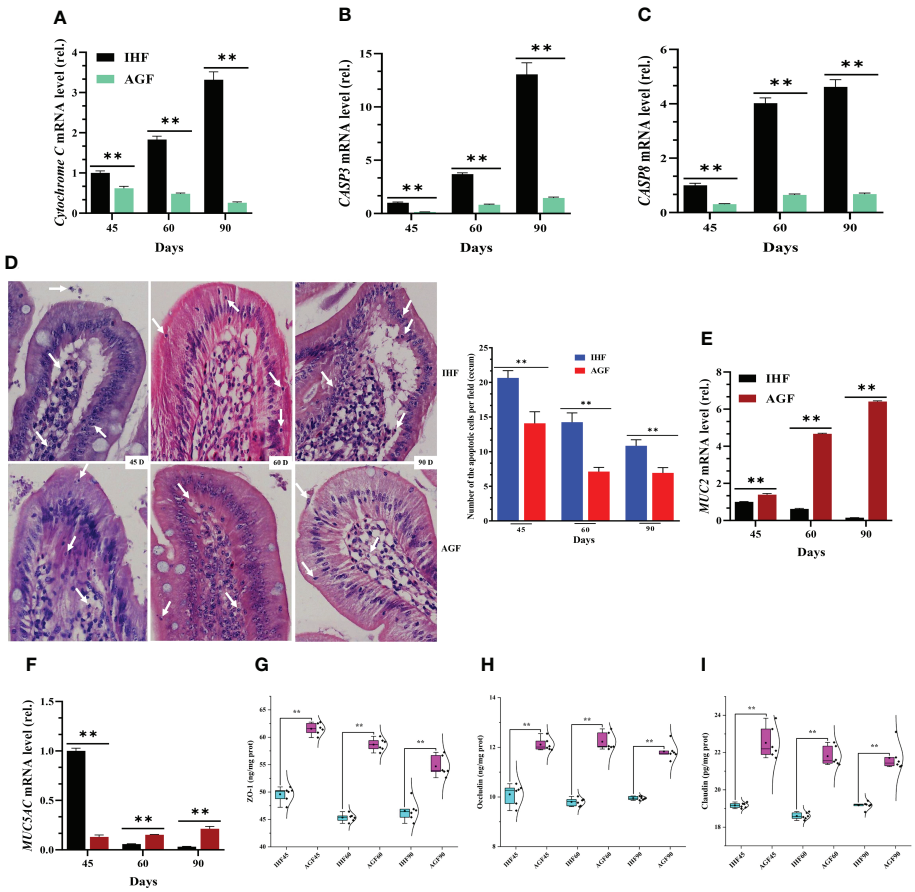

FIGURE 3
Beneficial effects of artificial pasture grazing system on in-house feeding system-dependent apoptosis-induced gut permeability in meat geese. **(A)** *Cytochrome C* mRNA level in cecal tissues, **(B)** *CASP3* mRNA level in cecal tissues, and **(C)** *CASP8* mRNA level in cecal tissues. **(D)** H&E staining of cecal tissues (magnification, 40×) for the number of apoptotic cells per field (Mean ± SD). **(E)** *MUC2* mRNA level in cecal tissues, and **(F)** *MUC5AC* mRNA level in cecal tissues, normalized by *β-actin* and measured by qPCR. **(G)** ZO-1 protein level in cecal tissues, **(H)** Occludin protein level in cecal tissues, and **(I)** Claudin protein level in cecal tissues. In-house feeding system (IHF) and artificial pasture grazing system (AGF). Data with different superscript letters are significantly different ($P < 0.05$) according to the unpaired student T-Test. The asterisks symbol indicates significant differences $^{**}P < 0.01$.

result was under reduced mRNA expression levels of *LC8* and *IkB-a* and increased mRNA levels of *NF-κB* in IHF meat geese (Figures 4A–C). Furthermore, we investigated the genes related to regulating NF-κB pathway. The mRNA expression of *NF-κB*-regulated genes *IL-8, CCL2, PLAU*, and *BIRC3* in IHF meat geese (Figures 4D) showed that *IL-8*, *PLAU*, and *BIRC3* were by far the most abundant contributor genes involved in regulating the NF-κB pathway in the cecal tissues of IHF meat geese. Further to confirm the NF-κB pathway activation in IHF meat geese, we performed the nuclear translocation of NF-κB by the immunofluorescence analysis. As observed using a confocal fluorescence microscope, most of the NF-κB protein was translocated into the cell nucleus in the cecal tissues of IHF meat geese compared with AGF meat geese (Figure 4E). Next, a significant increase in mRNA expression of pro-inflammatory mediators *iNOS* and *COX2* and cytokines *IL-1β, IL-6*, and *TNF-a* in cecal tissues of IHF meat geese were observed instead of *IL-1β* as a function of diet composition. Here we observed that intestinal ALP deficiency was associated with significantly increased mRNA expression levels of these five cytokines (Figures 4F–J).

Effects of artificial pasture grazing system on activation of Nrf2 pathway in meat geese

When NF-κB pathway is established under the insults of ROS, then a natural immune defense mechanism is activated underpinning the Keap1-Nrf2 pathway. *Keap1* regulates the activity of *Nrf2* and acts as a sensor for oxidative stress. Upon oxidative stress, *Keap1* loses its ability to ubiquitinate *Nrf2*, allowing *Nrf2* to move in the nucleus and activate its target genes

10.3389/fimmu.2022.1041070

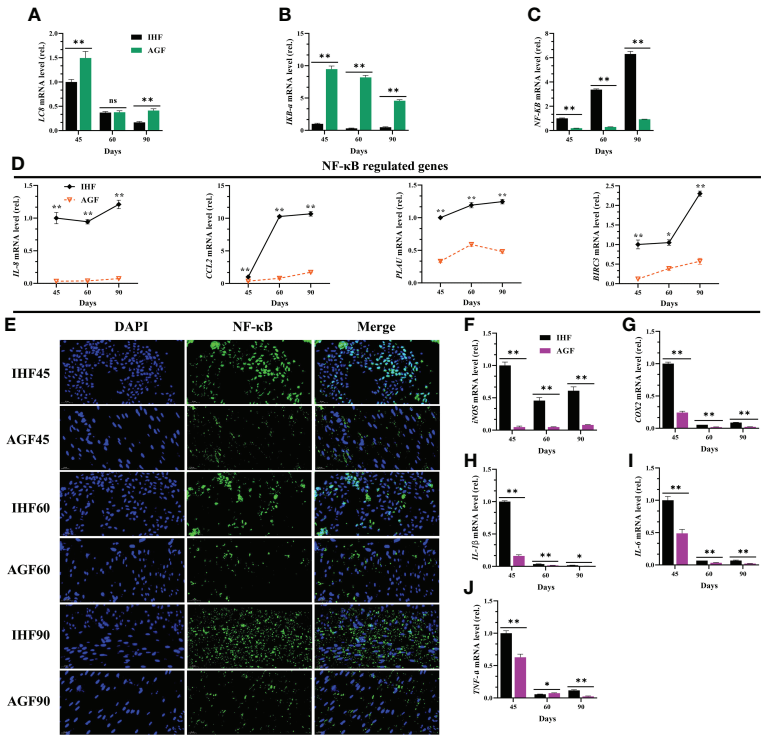

FIGURE 4
Inhibitory effects of artificial pasture grazing system on in-house feeding system-induced NF-κB pathway and its systemic inflammation. **(A)** *LC8* mRNA level in cecal tissues, **(B)** *IKB-a* mRNA level in cecal tissues, **(C)** *NF-κB* mRNA level in cecal tissues, **(D)** NF-κB-regulated genes (*IL-8, CCL2, PLAU,* and *BIRC3*) mRNA levels in cecal tissues, **(E)** Immunofluorescence (IF) analysis using Rabbit Anti-NF-κB (P65-AF5006) (1:200; v/v) showing nuclear translocation of NF-κB in the cecal tissues of meat geese. Blue: nucleus (DAPI); Green: NF-κB-staining; Cerulean blue: merge of blue and green indicating nuclear localization of NF-κB, scale bar = 20 μm. **(F)** *iNOS* mRNA level in cecal tissues, **(G)** *COX2* mRNA level in cecal tissues, **(H)** *IL-1β* mRNA level in cecal tissues, **(I)** *IL-6* mRNA level in cecal tissues, and **(J)** *TNF-a* mRNA level in cecal tissues, normalized by *β-actin* and measured by qPCR. In-house feeding system (IHF) and artificial pasture grazing system (AGF). Data with different superscript letters are significantly different ($P < 0.05$) according to the unpaired student T-Test. The asterisks symbol indicates significant differences $^{*}P < 0.05$, $^{**}P < 0.01$. The lack of a superscript letter means that all differences were nonsignificant (ns).

(47). For these consensus, first, we found that the mRNA expression levels of *Keap1* were declined and mRNA expression levels of *Nrf2* were increased by a limited ROS production in AGF meat geese (Figure 5A). This demonstrates that the production of ROS activates Nrf2 pathway. Because Nrf2 pathway is known to promote cellular redox homeostasis, and as the impairment of *Nrf2* activity is considered to play a crucial role in cellular defense system, we measured *Nrf2* and *Nrf2*-regulated genes and the antioxidant enzymes regulated by *Nrf2* in IHF and AGF meat geese at three-time points i.e. 45d, 60d, and 90d. With AGF system, the mRNA expression levels of *Nrf2* (Figure 5B) and *Nrf2*-regulated genes *NQ01, Gclc, Gclm*, and *GSTA4* were increased in AGF meat geese (Figure 5C). Next, to evaluate the impacts of AGF system on Keap1-Nrf2 pathway, we determined nuclear translocation of Nrf2 by immunofluorescence analysis. The results revealed increased Nrf2 in AGF versus IHF meat geese (Figure 5D), which suggested that artificial pasture intake may involve in the activation of the Nrf2 pathway. It is clearly understood that the improved Nrf2 regulation should contribute in antioxidant defense mechanisms. Again we observed that the pasture intake was involved in increased protein levels of antioxidants HO-1, GSR, T-SOD, GSH-PX, T-AOC, and CAT from serum samples of meat geese at 45d, 60d, and 90d (Figures 5E–J). Further, whether these antioxidants are involved in attenuating the mediators that caused ROS insults in IHF and AGF meat geese, we measured oxidative mediator MDA from serum samples. We examined a severe increase in protein levels of MDA in IHF meat geese compared with AGF meat geese at three time points 45d, 60d, and 90d (Figure 5K).

Artificial pasture grazing system attenuates the in-house feeding system-induced endotoxemia, gut permeability, and chronic systemic inflammation of meat geese

To further explore the effects of long-term establishment of AGF system on intestinal alterations at three-time points 45d,

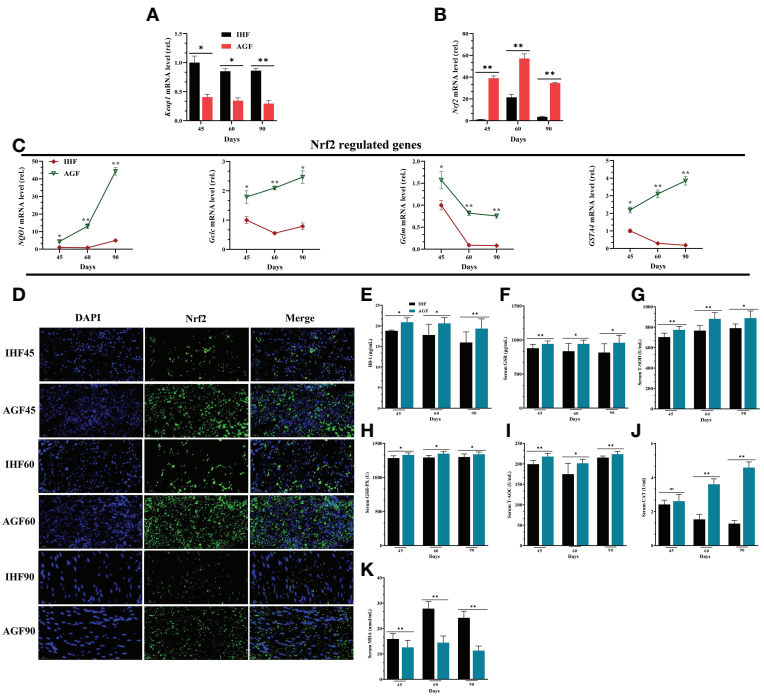

FIGURE 5
Effects of Artificial Pasture Grazing System on Activation of Nrf2 Pathway in Meat Geese **(A)** *Keap1* mRNA level in cecal tissues, **(B)** *Nrf2* mRNA level in cecal tissues, and **(C)** Nrf2-regulated genes (*NQO1, Gclc, Gclm*, and *GSTA4*) mRNA levels in cecal tissues, normalized by β-actin and measured by qPCR. **(D)** Immunofluorescence (IF) analysis using Rabbit anti-Nrf2 (bs1074R) (1:500; v/v) showing nuclear translocation of Nrf2 in the cecal tissues of meat geese. Blue: nucleus (DAPI); Green: Nrf2-staining; Cerulean blue: merge of blue and green indicating nuclear localization of Nrf2, scale bar = 20 μm. **(E)** HO-1 protein level **(F)** GSR protein level **(G)** T-SOD protein level **(H)** GSH-PX protein level **(I)** T-AOC protein level **(J)** CAT protein level and **(K)** MDA protein level. In-house feeding system (IHF) and artificial pasture grazing system (AGF). Data with different superscript letters are significantly different ($P < 0.05$) according to the unpaired student T-Test. The asterisks symbol indicates significant differences $^{*}P < 0.05$, $^{**}P < 0.01$.

60d, and 90d, we hypothesized whether intestinal ALP may involve in activating Nrf2 pathway, and we performed correlation analysis among host markers (Figure 9B). The results obtained from this relationship showed that intestinal ALP was positively correlated with *Nrf2* and *Nrf2*-regulated genes and as well as its antioxidant enzymes. Further Nrf2 pathway including its antioxidation immune system was positively correlated with *IL-4*, *IL-10*, and tight junction proteins including 2 genes encoding tight junction proteins *Discs large 1* (*dlg1*) and *E-cadherin*. IL4 and IL-10 are known to be anti-inflammatory cytokines (48). Indeed, we also measured the protein levels of cecal ALP by western blot analysis (Figure 6A) and by ELISA kit method (Figure 6B) in meat geese. The endotoxin (LPS) and ROS measured by ELISA kit method were increased in cecal tissues of IHF meat geese compared with AGF meat geese (Figures 6C, D). Further, we measured the mRNA expression levels of TJs proteins including *ZO-1*, *Occludin*, and *Claudin* (Figures 6E–G), 2 genes encoding tight junction proteins *dlg1* and *E-cadherin* (Figures 6H, I), anti-inflammatory cytokines (*IL-4* and *IL-10*) (Figures 6J, K), and pro-inflammatory cytokines (*iNOS*, *COX2*, *IL-1β*, *IL-6*, and *TNF-α*) (Figures 4F–J) in meat geese that have received AGF and IHF environment from 45d to 90d. The results obtained from correlation analysis suggest that the activation of Nrf2 pathway by intestinal ALP enzyme was primarily involved in attenuating endotoxemia, gut permeability, and pro-inflammatory cytokines in AGF meat geese.

Long-term artificial pasture grazing system attenuates the manifestation of *KEAP1*-induced aging phenotypes in meat geese

The investigation of impact of Nrf2 pathway activation on cecal tissues aging from the expression levels of aging marker genes showed elevated level of *p19ARF, p16INK4α*, and *p21* in IHF meat geese compared with cecal tissues of AGF meat geese at 45d, 60d, and 90d of age (Figures 7A–C). The results illustrated that Nrf2 pathway activation induced by ROS-directed *Keap1* inhibition effectively suppressed the manifestation of aging phenotypes in cecal tissues of AGF meat geese.

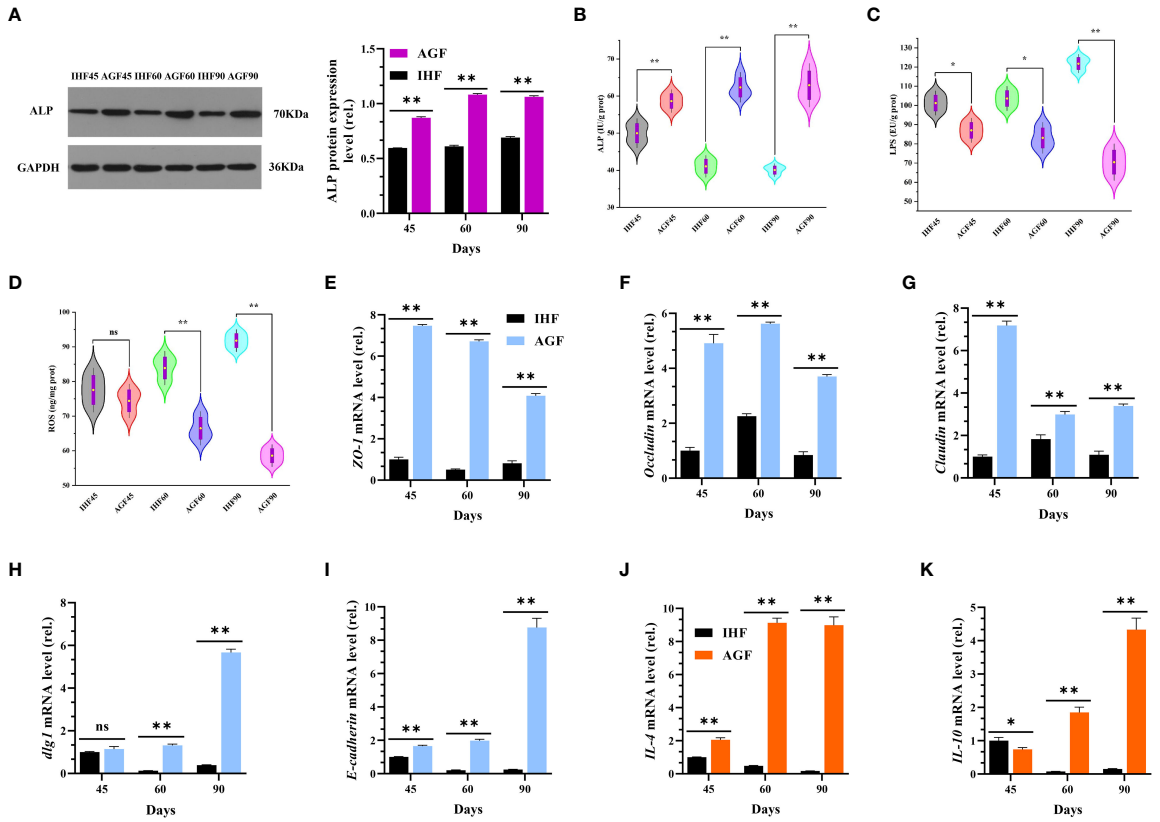

FIGURE 6
Artificial pasture grazing system attenuates the in-house feeding system-induced endotoxemia, gut permeability, and chronic systemic inflammation of meat geese. **(A)** Western blot analysis was performed to detect the protein levels of ALP in the cecal tissues, normalized by *GAPDH*. **(B)** ALP protein level in cecal tissues, **(C)** LPS protein level in cecal tissues, and **(D)** ROS protein level in cecal tissues. **(E)** *ZO-1* mRNA level in cecal tissues, **(F)** *Occludin* mRNA level in cecal tissues, **(G)** *Claudin* mRNA level in cecal tissues, **(H)** *dlg1* mRNA level in cecal tissues, **(I)** *E-cadherin* mRNA level in cecal tissues, **(J)** *IL-4* mRNA level in cecal tissues, **(K)** *IL-10* mRNA level in cecal tissues. In-house feeding system (IH) and artificial pasture grazing system (AGF). Data with different superscript letters are significantly different ($P < 0.05$) according to the unpaired student T-Test. The asterisks symbol indicates significant differences $^{*}P < 0.05$, $^{**}P < 0.01$. The lack of a superscript letter means that all differences were nonsignificant (ns).

Long-term artificial pasture grazing system improved metabolic profile in meat geese

The AGF system was effective in preventing metabolic syndrome in AGF meat geese with a significantly improved body weight (Figures 8A) and lipid profile (Figures 8B–E), as well as lowering blood glucose and urea nitrogen levels (Figures 8F, G).

Long-term Supplementation of artificial pasture grazing system impedes compositional changes in gut microbiota by stimulating intestinal ALP enzyme

The microbiota in meat geese' cecal chyme samples were analyzed at three time points (45d, 60d, and 90d) by deep sequencing of the bacteria 16S rRNA gene V3 – V4 region. As shown in Figure 9A, the Spearman correlation between microbiota and metabolic indices in the gut tract of meat geese at 45d showed significant positive association between *Bacteroides* with serum GSH-PX, and T-AOC and cecal ZO-1, Occludin, *IL-4*, *IL-10*, *LC8*, and *IKB-α* and negative association with serum LPS, ROS, T-AOC, and LDL-C, and cecal *NF-κB*, *TLR4*, *MyD88*, *COX2*, *IL-6*, *TNF-a*, *cytochrome C*, *CASP3*, *P16INK4α*, *P21*, body weight, and blood glucose. *Alistipes* were strongly positively correlated with the cecal pH, serum ALP, HO-1, GSH-PX, and T-AOC, and cecal Occludin, *IL-4*, *IL-10*, and *LC8* and negatively correlated with serum LPS, MDA, TCHO, TG, LDL-C, and ROS, and cecal *MyD88*, *NF-κB*, *TNF-a*, *cytochrome C*, *CASP3*, *p19ARF*, *p16INK4a*, *p21*, and blood glucose. *Lactobacillus* was positively correlated with serum ALP and HDL-C and cecal *Nrf2*, *IL-4*, ZO-1, Occludin, and *E- cadherin* and negatively correlated with serum LPS and TG, and cecal *LBP*, *sCD14*, *NF-κB*, *iNOS*, *IL-1β*, *cytochrome C*, *CASP3*, *Keap1*, *p19ARF*, *p16INK4a*, and *p21*. *Norank_f:norank_o:Gastranaerophilales* was positively correlated

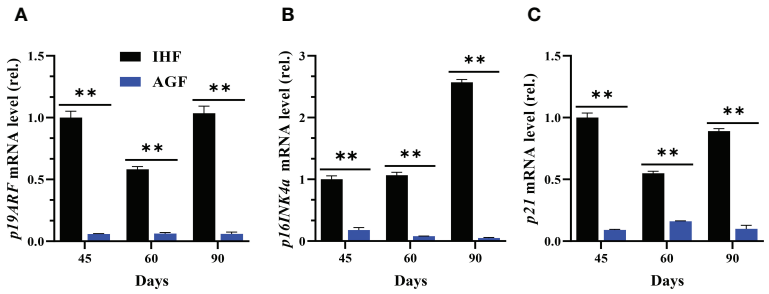

FIGURE 7
Effect of different feeding systems on KEAP1-induced aging phenotypes in meat geese. **(A)** *p19ARF* mRNA level in cecal tissues, **(B)** *p16INK4α* mRNA level in cecal tissues, and **(C)** *p21* mRNA level in cecal tissues, normalized by *β-actin* and measured by qPCR. In-house feeding system (IHF) and Artificial pasture grazing system (AGF). Data with different superscript letters are significantly different (P < 0.05) according to the unpaired student T-Test. The asterisks symbol indicates significant differences $^{**}P < 0.01$.

with serum T-AOC and cecal pH, Occludin, and *IL-4* and negatively correlated with serum LPS and cecal *iNOS*, *CASP3*, *Keap1*, *p19ARF*, and *p21*. *Alistipes* and *Lactobacillus* were strongly positively correlated with intestinal ALP and Nrf2 pathway and suppress all those bacteria (*Subdoligranulum*, *norank_f:norank_o:Clostridia_UCG_014*, and *Erysipelatoclostridium*) that were the causative factors for pathogenesis in AGF meat geese.

As diet has a major influence on gut microbiota composition, richness, and diversity (49). It has been known that the origin, type, and quality of diet modulate the gut microbiota in a time-dependent manner. Based on the previous studies, we hypothesized whether AGF system as a high dietary fiber source modulates the gut microbiota at different time points or not. We further analyzed the correlation between microbiota and metabolic indices in the gut tract of meat geese at 60d. The results of which showed that the *norank_f:norank_o:RF39* was significantly positively correlated with the cecal pH, serum HO-1 and GSH-PX and cecal *Nrf2*, *IL-4*, *IL-10*, Zo-1, Occludin, claudin, *dlg1*, and *E-cadherin* and negatively correlated with serum LPS and TG and cecal *MyD88*, *COX2*, *TNF-a*, *Keap1*, *p19ARF*, and *p16INK4a* in AGF meat geese. *Romboutsia* was positively correlated with cecal *Nrf2*, *IL-4*, *IL-10*, *dlg1*, *E-cadherin*, and *LC8* and negatively correlated with cecal *MyD88*, *iNOS*, *TNF-a*, and *p16INK4a*. *Norank_f:norank_o:RF39* and *Romboutsia* were positively correlated with Nrf2 pathway that was strongly involved in attenuating the harmful impacts of *Peptococcus* and *Ruminococcus_torques_group* in AGF meat geese.

To further illustrate the impacts of long-term establishment of AGF system on gut microbial modulation with different time

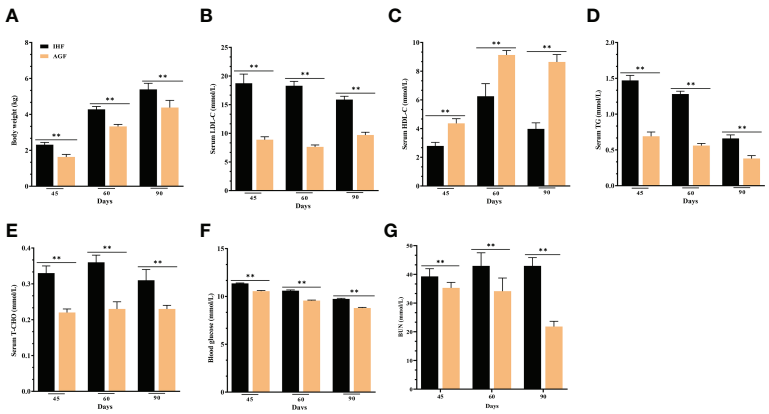

FIGURE 8
Effect of different feeding systems on metabolic profile of meat geese. **(A)** Body weight (kg), **(B)** LDL-C protein level in serum, **(C)** HDL-C protein level in serum, **(D)** TG protein level in serum, **(E)** T-CHO protein level in serum, **(F)** Blood glucose levels, and **(G)** BUN protein level in serum. In-house feeding system (IHF) and artificial pasture grazing system (AGF). Data with different superscript letters are significantly different (P < 0.05) according to the unpaired student T-Test. The asterisks symbol indicates significant differences $^{**}P < 0.01$.

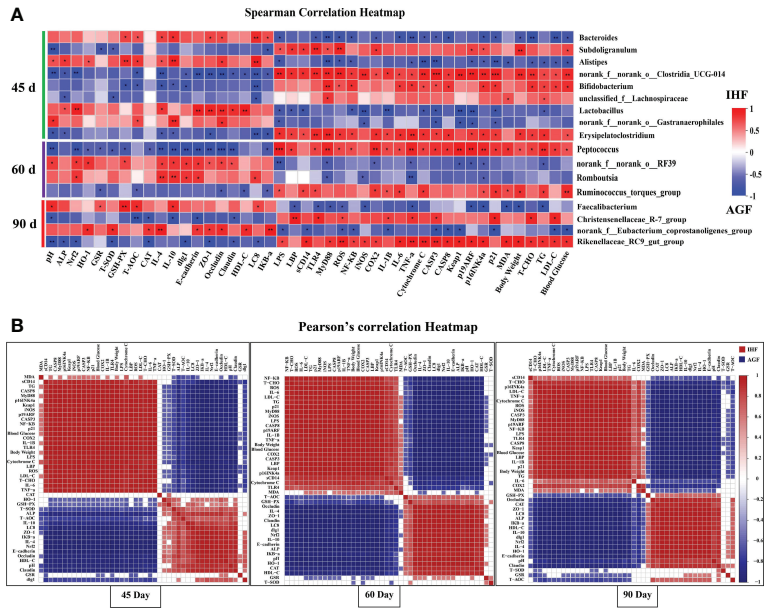

FIGURE 9
Association and model predictive analysis of the top 44 host markers with the highest correlation scores. **(A)** Correlation between gut microbiota and host markers by Spearman correlation analysis. Red squares indicate a positive correlation; whereas blue squares indicate a negative correlation. **(B)** The labels on the abscissa and the longitudinal axis represent Pearson's correlation heatmap among host markers. Red squares indicate a positive correlation and blue squares indicate a negative correlation. Deeper colors indicate stronger correlation scores. The asterisks symbol indicates significant differences *P < 0.05, **P < 0.01, ***P < 0.001.

points, we further started analyzing the correlation between microbiota and metabolic indices in the gut tract of meat geese at 90d. The results based on microbial alterations showed that *Faecalibacterium* was positively correlated with cecal pH, GSR, GSH-PX, and T-AOC and cecal *IL-10* and *LC8* and negatively correlated with serum ROS, MDA, and TG, and cecal *LBP*, *TLR4*, *MyD88*, *TNF-a*, *p19ARF*, and *p16INK4a*, and body weight. *Norank_f:Eubacterium_coprostanoligenes_group* was positively correlated with serum HO-1, T-SOD, CAT, and HDL-C and cecal *IL-4*, ZO-1, Occludin, *E-cadherin*, and *IKB-a* and negatively correlated with serum LPS, ROS, and LDL-C and cecal *sCD14*, *NF-κB*, *IL-1β*, *CASP3*, *CASP8*, *Keap1*, and *p21* and blood glucose. At 90 day we observed that *Faecalibacterium* was less positively correlated with ALP that detained the pathogenic effects of *Christensenellaceae_R-7_group* and *Rikenellaceae_RC9_gut_group* in AGF meat geese.

Next, a series of correlation analyses among endotoxemia, gut permeability, pro- and anti-inflammatory cytokines, aging phenotypes, and metabolic syndrome was shown by a Pearson's correlation heat map (Figure 9B) in meat geese at 45d, 60d, and 90d. Among them, *LBP* (P = 9.8E-08, R = 0.97351), *sCD14* (P = 1.4E-05, R = 0.92743), *TLR4* (P = 1E-08, R = 0.98324), *MyD88* (P = 3.2E-08, R = 0.97892), ROS (P = 4.6E-07, R = 0.96388), *NF-κB* (P = 3.4E-08, R = 0.97865), *cytochrome C* (P = 2.5E-07, R = 0.968042101), and *Keap1* (P = 2.8E-09, R = 0.98707) were significantly positively correlated with LPS at 45d in IH feeding meat geese. ALP (P = 0.00027, R = -0.8663), *Nrf2* (P = 2.7E-08, R = -0.9796), *IL-4* (P = 3E-07, R = -0.9669), *IL-10* (P = 2.8E-05, R = -0.9164), *dlg1* (P = 0.02022, R = -0.6572), *E-cadherin* (P = 4.4E-08, R = -0.9775), ZO-1 (P = 1.4E-06, R = -0.9546), Occludin (P = 2.6E-05, R = -0.9177), Claudin (P = 4.5E-06, R = -0.9426), *LC8* (P = 9.2E-06, R = -0.9334), and *IKB-a* (P = 1.5E-08, R = -0.9819) were negatively associated with LPS at 45d in GL feeding meat geese.

At 60d *LBP* (P = 1E-08, R = 0.98321), *sCD14* (P = 0.00011, R = 0.88818), *TLR4* (P = 0.00248, R = 0.78524), *MyD88* (P = 1.9E-11, R = 0.99523), ROS (P = 1.6E-09, R = 0.9885), *NF-κB* (P = 4.8E-07, R = 0.96351), *cytochrome C* (P = 0.00016, R = 0.88005), and *Keap1* (P = 1.2E-08, R = 0.98258) were significantly positively correlated with LPS in IH feeding meat geese. ALP (P = 9.2E-08, R = -0.9739), *Nrf2* (P = 1.3E-12, R = -0.9972), *IL-4* (P = 8E-12, R = -0.996), *IL-10* (P = 5E-13, R = -0.9977), *dlg1* (P = 5E-12, R = -0.9964), *E-cadherin* (P = 1.8E-13, R = -0.9981), ZO-1 (P = 5.1E-10, R = -0.9908), Occludin (P = 2.1E-08, R = -0.9806), Claudin (P = 5.5E-11, R = -0.9941), *LC8* (P = 1.6E-10, R = -0.9927), and *IKB-a* (P = 9.4E-07, R = -0.9582) were negatively associated with LPS at 60d in GL feeding meat geese.

At 90d *LBP* (P = 3.2E-10, R = 0.99164), *sCD14* (P = 0.01474, R = 0.68113), *TLR4* (P = 1E-10, R = 0.99336), *MyD88* (P = 4.8E-12, R = 0.99638), ROS (P = 4.6E-10, R = 0.99098), *NF-κB* (P = 2.1E-08, R = 0.98056), *cytochrome C* (P = 5.8E-09, R = 0.98501), and *Keap1* (P = 2.4E-09, R = 0.98744) were

significantly positively correlated with LPS in IH feeding meat geese. ALP (P = 1E-08, R = -0.9832), *Nrf2* (P = 2.2E-11, R = -0.9951), *IL-4* (P = 7.2E-12, R = -0.9961), *IL-10* (P = 9.6E-11, R = -0.9934), *dlg1* (P = 6.7E-10, R = -0.9903), *E-cadherin* (P = 1.3E-11, R = -0.9956), ZO-1 (P = 4.5E-12, R = -0.9964), Occludin (P = 5.5E-06, R = -0.94), Claudin (P = 1.3E-05, R = -0.9285), *LC8* (P = 9.1E-11, R = -0.9935), and *IKB-a* (P = 2.2E-08, R = -0.9803) were negatively associated with LPS at 60d in GL feeding meat geese.

Discussion

Intracellular ROS production by diet-induced gut microbiota facilitated LPS generation (50) may lead to chronic low-grade inflammation and modern chronic inflammatory diseases (51). Discovering a safe and novel means of limiting its development is urgently required for the prevention and treatment of these diseases. Diet is a primordial need for life and today, the modern poultry industry is based on grains with lower content of dietary fiber (52). Moreover, the worldwide trends of excessive low dietary fiber intake have been implicated in today's chronic inflammatory diseases including diabetes mellitus, autoimmune, cancer, cardiovascular, and chronic kidney disease (53, 54). However, the connections between the shifts in dietary fiber contents and attenuating the incidence of chronic inflammatory diseases by activating the intestinal ALP-dependent-redox signaling mechanism remain to be elucidated in meat geese. Therefore the present study demonstrates for the first time, that a long-term pasture grazing can alleviate commercial diet-induced gut microbial dysbiosis, gut barrier dysfunction and integrity, inflammatory diseases, aging phenotypes, and metabolic syndrome.

Though recent dietary supplementation studies have addressed some impacts of dietary fiber on gut microbiota (55, 56). However, despite these captivating findings, the mechanisms underlying these diverse associations and their outcomings have not been fully explored. In our study, we established artificial pasture grazing system for meat geese that supports concurrent processes to impede in-house feeding system-induced metabolic endotoxemia and systemic inflammation. Consequently, the innovative feature of the AGF system as a high dietary fiber source is to build a pathway-based mechanism by which it increased the abundance of intestinal ALP-producing bacteria, and prevented IHF system-induced LPS-producing bacteria. These changes improve the intestinal nutrient absorption, mucus layer, and mucus-producing goblet cell genes, resulting in reduced metabolic endotoxemia (LPS), LPS-induced ROS production, and gut permeability. The subsequent reduction of pro-inflammatory cytokines lead to the prevention of chronic inflammatory diseases and aging phenotypes. Spearman and Pearson's correlation analysis, including the above-mentioned findings, strongly supports the proposed mechanisms.

Metabolic endotoxemia can be determined by the abundance of bacteria affecting LPS production (57). In this study, we found that AGF intervention reduced the enrichment of genes involved in LPS biosynthesis based on the predicted function by 16S rRNA sequencing and PICRUSt analysis. Interestingly, our current findings have shown similar results with AGF intervention similar to dietary capsaicin in human subjects (58). This would indicate the possibility that a lower abundance of Gram-negative microbiota must be responsible for the low abundance of COG orthology belonging to LPS biosynthesis functions in the AGF meat geese. This could mainly be due to the prevention of members of the Gram-positive phyla *Firmicutes* (genera *Lactobacillus*, *Ruminococcus_torques_group*, *Subdoligranulum*, and *Christensenellaceae_R-7_group*) and *Actinobacteriota* (genera *norank_f_norank_o_Gastranaerophilales*) and gram-negative phyla *Bacteroidota* (genera *Prevotellaceae_UCG_001*, *Bacteroides*, *Alistipes*, and *Rikenellaceae_RC9_gut_group*) with AGF intervention because these were the key bacterial phyla and their respective genera that largely contribute to the IHF meat geese. These lipopolysaccharides are bacterium-associated molecular patterns, which act *via* TLR4/MyD88 pathway by promoting the inflammatory response (59).

The production of ROS by LPS-induced TLR4/MyD88 pathway activation (44) may depend on a diet rich in high fat, high calorie, high protein, and high carbohydrates (60, 61). The correct cellular response to ROS production is critical to preventing oxidative damage and maintaining cell survival. However, when too much cellular damage has occurred, it is to the advantage of a multicellular organism to remove the cell for the benefit of the surrounding cells. ROS can therefore trigger apoptotic cell death based on the severity of the oxidative stress (62) and may contribute to inducing NF-κB pathway (63). ROS-induced severe apoptotic cell death may accelerate intestinal mucosa disruption and result in causing intestinal permeability (64). Based on the current studies, we hypothesized how intestinal ALP would incinerate in LPS-induced TLR4/MyD88 facilitates ROS production pathway.

Intestinal ALP is a major enzyme of interest for its gut microbiota-modifying properties (65, 66). Endogenous ALP production has been shown to inhibit the overgrowth of *E. coli* by dephosphorylating LPS (28, 57, 67). It is well known that intestinal ALP capacity to dephosphorylate LPS was shown to be present in the colon and feces of mice (26) and reduces LPS-induced gut permeability and inflammation in Caco2 and T84 cell lines (68). LPS binds specifically to TLR4 and stimulates inflammation by activating two distinct pathways, namely LPS-dependent release of TNF-α and NF-κB (through MyD88-dependent and –independent pathways) (69). The data from our experiment support the notion that the AGF system as high

dietary fiber source enhanced the abundance of intestinal ALP producing *Alistipes*, and *Lactobacillus*, (45d), *Norank_f: norank_o:RF39* and *Romboutsia* (60d), and *Faecalibacterium* (90d) genera. This microbiota was further seen to involve in suppressing *E. coli* and inactivating the capacity of lipid A biosynthesizing genes (*lpxA*, *lpxB*, *lpxC*, and *lpxD*) to bind LPS with TLR4 and then inhibit the activation ability of MyD88 dependent pathway. Some reports, utilizing dietary fiber as a nutrient source in animals, support our results (24, 70).

It is well-known that endogenous ALP production enhances the expression of proteins (Zo-1, Occludin, and Claudin) involved in tight junctions, thereby preventing the translocation of endotoxins (LPS) by intestinal gram-negative bacteria (*E. coli*) across the gut barrier (21, 57). Our results were by the reports of Kaliannan et al. (57); Schroeder et al. (71); Kühn et al. (21); and Mei et al. (72), in which microbially-induced endogenous intestinal ALP production was observed to decrease the ROS production and apoptosis-related genes *CASP3* and *CASP8*, improve the mucus-producing goblet cell genes *MUC2* and *MUC5AC* as well as inner muscular tonic/muscularis mucosal layer thickness. Moreover, tight junction proteins Zo-1, Occludin, and Claudin and 2 genes encoding tight junction protein *dlg1* and *E-cadherin* were observed to be increased in AGF meat geese which gave the fact that these proteins were strongly involved in inducing nutrient absorption and overall intestinal health (Figure 10).

ROS production regulates *NF-κB* activity in a bidirectional fashion, namely, ROS may trigger activation or repression of *NF-κB* activity (73). In many studies, *NF-κB* inhibition is LC8 dependent (46). But in our study, we have shown that the activation of *NF-κB* by LPS-induced TLR4/MyD88-accelerated ROS production is collectively *LC8* and *IkB-a* dependent. Some reports, utilizing LPS as a ROS inducer, support our results (74, 75). The results of our study with a little modification from those of Cario (76) and Fukata et al. (69), evinced that the triggering of LPS facilitated MyD88 pathway and the subsequent ROS production may altogether activate the *NF-κB* signaling cascades, which played an important role in the development of inflammation by synthesizing and stimulating pro-inflammatory cytokines (*iNOS*, *COX2, IL-1β, IL-6*, and *TNF-α*) (29, 77). Dysregulated inflammatory cytokines production plays a pivotal role in developing low-grade inflammation (78). The above-mentioned so-called studies were unable to describe whether the activation of NF-κB pathway and the resulted pro-inflammatory cytokines were owing to connections between the dietary components (dietary fiber) and gut microbiota. Our results were in accordance with the report of Kyung-Ah Kim et al. (79); Eva d'Hennezel et al. (5); and Sun et al. (51) in which the microbially-induced LPS production increased the mRNA expression of *NF-κB, iNOS, COX2, IL-1β, IL-6*, and *TNF-α* in the liver of mice, pigs, and humans as that of our IHF treatment meat geese. Conversely, in our study, we discovered from the spearman correlation analysis between microbiota and host markers that AGF intervention prevented the IHF-induced upregulation of gut microbiota interacting with LPS, ROS, and pro-inflammatory cytokines by activating gut microbiota those directly interacting with intestinal ALP and Nrf2 pathway. Further, following the mechanism of Bates et al. (80) and Estaki et al. (28), we developed combined Pearson's correlation analysis among host markers to evaluate whether intestinal ALP is involved in activating Nrf2 pathway. We observed that the intestinal ALP was significantly positively correlated with Nrf2 in all stages of sample collection suggesting that intestinal ALP may contribute to activating Nrf2 pathway in AGF treatment meat geese.

In response to oxidative challenge, a stress response is activated to control ROS overproduction and provide optimal conditions for effective ROS signaling to support redox homeostasis. The Nrf2/Keap1 and nuclear factor kappa-light-chain-enhancer of activated B cells/inhibitory κB protein (NF-κB/IkB) systems were considered to be two major "master regulators" of the stress response. One of the most important ways in which *NF-κB* activity influences ROS levels is *via* increased expression of antioxidant proteins has been explained elsewhere (81). The way by which Keap1-Nrf2 responds to ROS has not been elucidated clearly in meat geese. Upon oxidative stress, *Keap1* acts as a sensor and regulates the activity of *Nrf2* thereby, *Keap1* loses its ability to ubiquitinate *Nrf2*, allowing *Nrf2* to move in the nucleus and activate its target genes (47, 82). The results of our study following this mechanism by which dietary fiber in AGF meat geese was able to activate intestinal ALP that was significantly positively correlated with *Nrf2* and *Nrf2*-regulated genes including *NQ01, Gclc, Gclm*, and *GSTA4*, and the antioxidant defense network-related enzymes such as HO-1, GSR, T-SOD, GSH-PX, T-AOC, and CAT and significantly negatively correlated with oxidative related enzyme MDA.

Several studies revealed that *Nrf2* activity is modulated with different dietary interventions such as a high-fat diet or dietary energy restriction (83, 84). The results suggest that the progression of age-related phenotypes *p19ARF, p16INK4α*, and *p21* detected in this study are primarily caused by the decline of protective function by Nrf2 pathway in IHF meat geese. This may be because of chronic smoldering inflammation which is considered one of the important factors associated with low-fiber diet-related diseases and aging phenotypes (53, 85). We indeed observed that the expression of pro-inflammatory cytokine genes *iNOS, COX2, IL-1β, IL-6*, and *TNF-a* were increased in IHF meat geese. While epidemiological evidence shows that *TNF-a* and *IL-6* are predictive of many aging phenotypes (86). Hence, we found it to be associated with more pronounced aging phenotypes *p19ARF, p16INK4α*, and

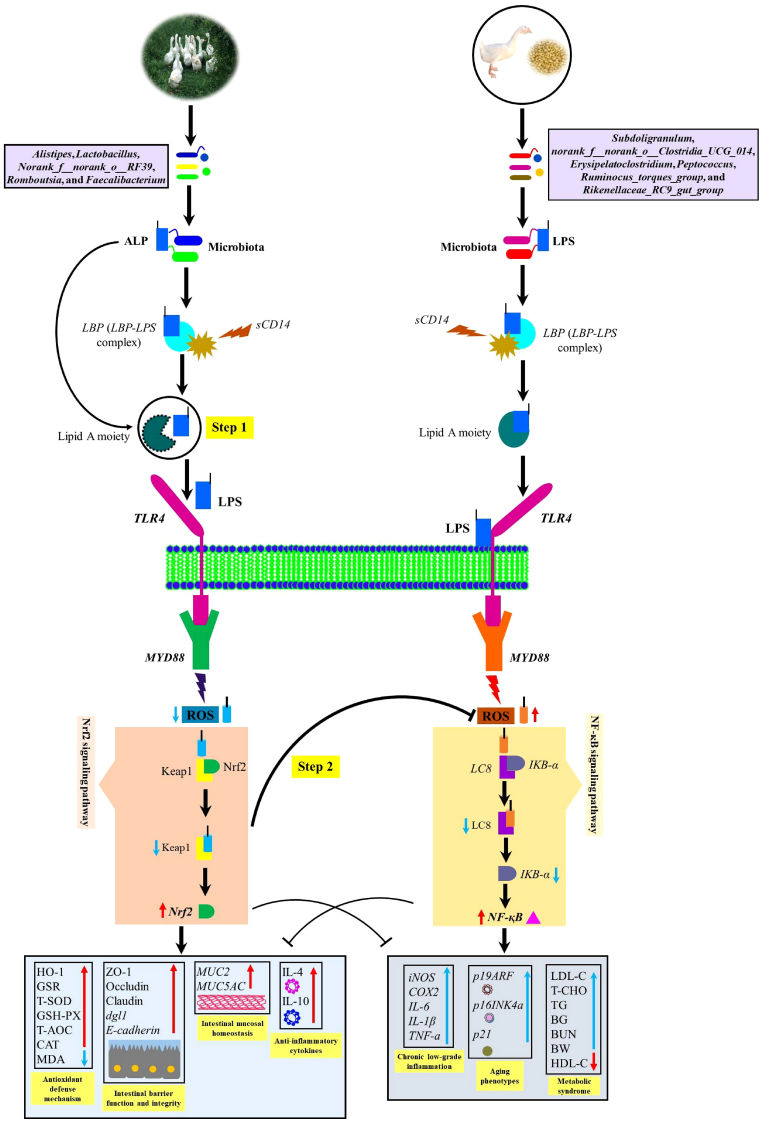

FIGURE 10
Diagram illustrating a proposed mechanism by which artificial pasture grazing system as a high dietary fiber source up-regulates intestinal ALP-producing bacteria and Nrf2 signaling pathway while downregulating LPS-producing bacteria and ROS in meat geese. The increase in intestinal ALP-producing bacteria and the activation of Nrf2 signaling pathway maintain antioxidant and anti-inflammatory mechanisms that lower LPS-producing bacteria and LPS-induced ROS generation, intestinal mucosal deterioration, gut permeability, and metabolic endotoxemia. In the first step, the intestinal ALP attack on TLR4 and let the lipid A moiety not to allow LPS to bind with TLR4 and dephosphorylate LPS by breaking TLR4/MyD88-induced ROS production. In the second step, intestinal ALP activates Nrf2 pathway which reduces oxidative stress, so that ROS could not oxidize LC8 protein and deteriorate IKB-a to activate NF-κB pathway. In this way, intestinal ALP activates anti-inflammatory cytokines and then attenuates chronic low-grade inflammation, aging phenotypes, and metabolic syndrome. BG, blood glucose; TG, triglyceride; BW, body weight; BUN, blood urea nitrogen.

p21 in geese lacking pasture intake, whereas long-term AGF system significantly induced the potent anti-inflammatory action of *Nrf2* and it may evolve in reducing the pro-inflammatory cytokines in AGF meat geese with concomitantly, aging phenotypes. Of note, our results suggest that AGF-induced intestinal ALP positively correlates with *Nrf2* and negatively correlates with *Keap1* and pro-inflammatory cytokines. This notion coincides with the fact that *Nrf2*-mediated inhibition of *iNOS*, *COX2*, *IL-1β*, *IL-6*, and *TNF-a* induction contributes to the prevention of delayed aging phenotypes (87) and the development of geese' health.

In a previous study, intestinal ALP regulation prevents and reverses the changes associated with a high-fat diet-induced metabolic syndrome (21). Furthermore, regulation of intestinal

ALP by dietary fiber-rich diets improves the lipid profile during low dietary fiber and low-fat diets (88). In the current study, we found a low dietary fiber-related spontaneous increase in the serum lipid profile and glucose levels in meat geese, significantly more pronounced in geese lacking pasture intake, underscoring the potential beneficial role of AGF-induced intestinal ALP in the prevention of metabolic diseases.

To prove the hypothesis that intestinal ALP might directly contribute to the reduction of endotoxemia, gut permeability, pro-inflammatory cytokines, and metabolic syndrome, we applied a combined correlation analysis among them. We found that ROS production owing to microbially-induced LPS was seen to be increased with IHF system and further involved in inducing intestinal mucosa deterioration, apoptosis, gut permeability, oxidants, NF-κB pathway, pro-inflammatory cytokines, aging phenotypes, and metabolic syndrome. The establishment of AGF system as a high dietary fiber source can reverse this process. Specifically, AGF system increase the abundance of ALP-producing bacteria and that intestinal ALP negatively correlates with ROS. The low production of ROS in AGF meat geese interacts with *Keap1* and diminishes its activity and then alternatively activates the Nrf2 pathway. Activation of intestinal ALP and Nrf2 pathway collectively positively correlates with *LC8*, *IKB-a*, antioxidants (HO-1, GSR, T-SOD, GSH-PX, CAT, and T-AOC), tight junction proteins ZO-1, Occludin, and Claudin, including 2 genes encoding tight junction proteins *dlg1* and *E-cadherin*, and anti-inflammatory cytokines (*IL-4* and *IL-10*). *IL-4* is produced by Th2 cells (89) whereas *IL-10* is involved in Th2 differentiation (90) and both are known to be anti-inflammatory cytokines (48). Several pieces of evidence from previous studies revealed that *IL-4* and *IL-10* depletion is associated with pronounced ulcerative colitis and Crohn's disease, type 2 diabetes, metabolic syndrome (91, 92). In our study, the activation of intestinal ALP, Nrf2 pathway, antioxidants, *IKB-a*, and anti-inflammatory cytokines potentially evolve in reducing endotoxemia, gut permeability, pro-inflammatory cytokines, aging phenotypes, and metabolic syndrome in AGF meat geese.

In summary, our data suggest that intestinal ALP – as a natural brush border enzyme – plays a critical role in animal health development through maintaining intestinal microbiome homeostasis, reducing LPS-induced ROS production, activating Nrf2 pathway, inducing anti-inflammatory immune responses, and preserving gut barrier function, decreasing low-grade inflammation, and metabolic syndrome. Further studies will focus on elucidating the precise mechanisms of intestinal ALP and Nrf2 pathways' beneficial role in different dietary patterns and aging. Given that AGF system safely induces intestinal ALP and Nrf2 pathways, targeting specific dietary fiber sources that could induce endogenous intestinal ALP production could represent a novel approach to preventing a variety of diet-induced gut microbial-related diseases in animals.

Conclusions

In conclusion, microbially-induced ALP production by AGF system appears to preserve intestinal microbial homeostasis by targeting crucial intestinal alterations, including LPS-induced ROS, gut barrier dysfunction, systemic chronic low-grade inflammation, and metabolic syndrome. By targeting specific dietary fiber sources that could induce endogenous intestinal ALP production may represent a novel therapy to counteract the chronic inflammatory state leading to low dietary fiber-related diseases in animals. If confirmed in humans, these findings may help to better understand diseases with an affected gut barrier functions, such as obesity, ulcerative colitis, cardiovascular, and Crohn's disease.

Data availability statement

Sequence data for cecal microbiome has been uploaded in Sequence Read Achrive of NCBI under accession code: SRP395138.

Ethics statement

The animal study was reviewed and approved by Henan Agricultural University (approval HENAU-2021).

Author contributions

QA and SM designed research, conducted experiments, acquired data, analyzed data, performed statistical analysis, and wrote the manuscript. JN, FL, DL, ZW, HS, and YC acquired data and conducted experiments. YS, SM, and UF designed research, analyzed data, and critically revised the manuscript for intellectual content. All authors contributed to the article and approved the submitted version.

Funding

This work was supported by grants from the Modern Agro-industry Technology Research System of China (CARS-34) and the Science and Technology Innovation Team of Henan Province High Quality Forage and Animal Health (No.22IRTSTHN022).

Acknowledgments

We thank Henan Daidai goose Agriculture and Animal husbandry development Co. LTD (Zhumadian, China) for

providing Wanfu meat geese stocks used in this study. We thank Shi yinghua and San Ma for assistance with microbiome analysis.

Conflict of interest

The authors declare that the research was conducted in the absence of any commercial or financial relationships that could be construed as a potential conflict of interest.

Publisher's note

All claims expressed in this article are solely those of the authors and do not necessarily represent those of their affiliated organizations, or those of the publisher, the editors and the reviewers. Any product that may be evaluated in this article, or claim that may be made by its manufacturer, is not guaranteed or endorsed by the publisher.

Supplementary material

The Supplementary Material for this article can be found online at: https://www.frontiersin.org/articles/10.3389/fimmu.2022.1041070/full#supplementary-material. The supplementary materials are available from FigShre: http://doi.org/10.6084/m9.figshare.21543024.

SUPPLEMENTAL FIGURE 1
Overview of feeding and sampling strategies.

SUPPLEMENTAL FIGURE 2
Contributions of bacteria at phylum level to LPS biosynthesis functions. **(A–F)** Relative abundances (%) of the six most dominant phyla in the cecal chyme of the IHF and AGF meat geese. Data with different superscript letters are significantly different (P < 0.05) according to the unpaired student T-Test. *P < 0.05, **P < 0.01.

SUPPLEMENTAL FIGURE 3
Contribution of individual genera within each phylum to LPS biosynthesis functions. The complete name for each genus is given below. **(A)** Relative abundances (%) of the sixteen most dominant genera (*Subdoligranulum, norank_f:norank_o:Clostridia_UCG-014, unclassified_f:Lachnospiraceae, Lactobacillus, Faecalibacterium, Erysipelatoclostridium, Ruminococcus_torques_group, unclassified_f:Oscillospiraceae, Faecalitalea, Peptococcus, Blautia, Romboutsia, Christensenellaceae_R-7_group, norank_f:Eubacterium_coprostanoligenes_group, Enterococcus, Butyricicoccus*, and *norank_f:norank_o:RF39*) within phylum Firmicutes in the cecal contents of the IHF and AGF meat geese. **(B)** Relative abundances (%) of the five most dominant genera (*Bacteroides, Alistipes, Parabacteroides, Prevotellaceae_UCG-001*, and *Rikenellaceae_RC9_gut_group*) within phylum Bacteroidota in the cecal contents of the IHF and AGF meat geese. **(C–E)** Relative abundances (%) of the most dominant genera within phylum Actinobacteriota (Bifidobacterium), Cyanobacteria (norank_f:norank_o:Gastranaerophilales), and Desulfobacterota (Desulfovibrio) in the cecal chyme of the IHF and AGF meat geese. Data with different superscript letters are significantly different (P < 0.05) according to the unpaired student T-Test. *P < 0.05, **P < 0.01.

SUPPLEMENTAL FIGURE 4
Effect of different feeding systems on pH values of meat geese gastrointestinal tract. **(A)** pH of proventriculus, **(B)** pH of gizzard, **(C)** pH of ileum, and **(D)** pH of cecum. In-house feeding system (IHF) and artificial pasture grazing system (AGF). Data with different superscript letters are significantly different (P < 0.05) according to the unpaired student T-Test. The asterisks symbol indicates significant differences *P < 0.05, **P < 0.01.

SUPPLEMENTAL FIGURE 5
Effects of different feeding systems on *E. coli* production in cecal tissues of meat geese. **(A)** Representative culture plate photos showing the difference between IHF and AGF meat geese in the growth of LPS-producing gram-negative *E. coli*. CFU/g stool. **(B)** *E. coli* cell cultures based on spectrophotometer readings at OD600 for 48h. Data with different superscript letters are significantly different (P < 0.05) according to the unpaired student T-Test. *P < 0.05, **P < 0.01.

SUPPLEMENTAL FIGURE 6
Effects of different feeding systems on cecal morphology (100μm). VH – villus height; VW – villus width; DBV – distance between two villi; CD – crypt depth. In-house feeding system (IHF) and artificial pasture grazing system (AGF).

SUPPLEMENTAL FIGURE 7
(A) Comparison of the goblet cell number (per 20μm) of meat geese with different feeding systems. H&E staining of cecal tissues (magnification, 40×). Goblet cell (GC), In-house feeding system (IHF) and artificial pasture grazing system (AGF). Data with different superscript letters are significantly different (P < 0.05) according to the unpaired student T-Test. The asterisks symbol indicates significant differences *P < 0.05, **P < 0.01.

SUPPLEMENTAL FIGURE 8
(A) Light micrograph of the wall of cecum tissues of meat geese, hematoxylin and eosin (40μm): *1* – outer layer of muscular tonic; *2* – inner layer of muscular tonic; *3* – outer layer of lamina muscularis mucosa (LMM); *4* – submucosal nerve node; and *5* – inner layer of lamina muscularis mucosa (LMM). **(B)** Comparison of the cecal membrane thickness of meat geese with different feeding systems (50μm). In-house feeding system (IHF) and artificial pasture grazing system (AGF).

References

1. Mishra B, Jha R. Oxidative stress in the poultry gut: Potential challenges and interventions. *Front Vet Sci* (2019) 6:60. doi: 10.3389/fvets.2019.00060

2. Sperandeo P, Martorana AM, Polissi A. Lipopolysaccharide biogenesis and transport at the outer membrane of gram-negative bacteria. *Biochim Biophys Acta Mol Cell Biol Lipids* (2017) 1862:1451–60. doi: 10.1016/j.bbalip.2016.10.006

3. Moreira AP, Texeira TF, Ferreira AB, Peluzio Mdo C, Alfenas Rde C. Influence of a high-fat diet on gut microbiota, intestinal permeability and metabolic endotoxaemia. *Br J Nutr* (2012) 108:801–9. doi: 10.1017/S0007114512001213

4. Weise G, Drews G, Jann B, Jann K. Identification and analysis of a lipopolysaccharide in cell walls of the blue-green alga anacystis nidulans. *Archiv für Mikrobiologie* (1970) 71:89–98. doi: 10.1007/BF00412238

5. D'hennezel E, Abubucker S, Murphy LO, Cullen TW. Total lipopolysaccharide from the human gut microbiome silences toll-like receptor signaling. *mSystems* (2017) 2(6):e00046–17. doi: 10.1128/mSystems.00046-17

6. Huisman J, Codd GA, Paerl HW, Ibelings BW, Verspagen JMH, Visser PM. Cyanobacterial blooms. *Nat Rev Microbiol* (2018) 16:471–83. doi: 10.1038/s41579-018-0040-1

7. Williams JM, Duckworth CA, Burkitt MD, Watson AJ, Campbell BJ, Pritchard DM. Epithelial cell shedding and barrier function: a matter of life and death at the small intestinal villus tip. *Vet Pathol* (2015) 52:445–55. doi: 10.1177/0300985814559404

8. Awad WA, Hess C, Hess M. Enteric pathogens and their toxin-induced disruption of the intestinal barrier through alteration of tight junctions in chickens. *Toxins (Basel)* (2017) 9(2):60. doi: 10.3390/toxins9020060

9. Park CM, Park JY, Noh KH, Shin JH, Song YS. Taraxacum officinale weber extracts inhibit LPS-induced oxidative stress and nitric oxide production *via* the NF-κB modulation in RAW 264.7 cells. *J Ethnopharmacol* (2011) 133:834–42. doi: 10.1016/j.jep.2010.11.015

10. Jiang J, Yin L, Li JY, Li Q, Shi D, Feng L, et al. Glutamate attenuates lipopolysaccharide-induced oxidative damage and mRNA expression changes of tight junction and defensin proteins, inflammatory and apoptosis response signaling molecules in the intestine of fish. *Fish Shellfish Immunol* (2017) 70:473–84. doi: 10.1016/j.fsi.2017.09.035

11. Bishop RE. Fundamentals of endotoxin structure and function. *Contrib Microbiol* (2005) 12:1–27. doi: 10.1159/000081687

12. Kwon DH, Cha HJ, Choi EO, Leem SH, Kim GY, Moon SK, et al. Schisandrin a suppresses lipopolysaccharide-induced inflammation and oxidative stress in RAW 264.7 macrophages by suppressing the NF-κB, MAPKs and PI3K/Akt pathways and activating Nrf2/HO-1 signaling. *Int J Mol Med* (2018) 41:264–74. doi: 10.3892/ijmm.2017.3209

13. Kolodkin AN, Sharma RP, Colangelo AM, Ignatenko A, Martorana F, Jennen D, et al. ROS networks: designs, aging, parkinson's disease and precision therapies. *NPJ Syst Biol Appl* (2020) 6:34. doi: 10.1038/s41540-020-00150-w

14. Katsori AM, Palagani A, Bougarne N, Hadjipavlou-Litina D, Haegeman G, Vanden Berghe W. Inhibition of the NF-κB signaling pathway by a novel heterocyclic curcumin analogue. *Molecules* (2015) 20:863–78. doi: 10.3390/molecules20010863

15. Lazar V, Ditu L-M, Pircalabioru GG, Gheorghe I, Curutiu C, Holban AM, et al. Aspects of gut microbiota and immune system interactions in infectious diseases, immunopathology, and cancer. *Front Immunol* (2018) 9. doi: 10.3389/fimmu.2018.01830

16. Tang J, Xu L, Zeng Y, Gong F. Effect of gut microbiota on LPS-induced acute lung injury by regulating the TLR4/NF-kB signaling pathway. *Int Immunopharmacol* (2021) 91:107272. doi: 10.1016/j.intimp.2020.107272

17. Fan MZ, Archbold T. Novel and disruptive biological strategies for resolving gut health challenges in monogastric food animal production. *Anim Nutr* (2015) 1:138–43. doi: 10.1016/j.aninu.2015.10.002

18. Wellington MO, Hamonic K, Krone JEC, Htoo JK, Van Kessel AG, Columbus DA. Effect of dietary fiber and threonine content on intestinal barrier function in pigs challenged with either systemic e. coli lipopolysaccharide or enteric salmonella typhimurium. *J Anim Sci Biotechnol* (2020) 11:38. doi: 10.1186/s40104-020-00444-3

19. Sahasrabudhe NM, Beukema M, Tian L, Troost B, Scholte J, Bruininx E, et al. Dietary fiber pectin directly blocks toll-like receptor 2-1 and prevents doxorubicin-induced ileitis. *Front Immunol* (2018) 9:383. doi: 10.3389/fimmu.2018.00383

20. Chauhan A, Islam AU, Prakash H, Singh S. Phytochemicals targeting NF-κB signaling: Potential anti-cancer interventions. *J Pharm Anal* (2022) 12:394–405. doi: 10.1016/j.jpha.2021.07.002

21. Kühn F, Adiliaghdam F, Cavallaro PM, Hamarneh SR, Tsurumi A, Hoda RS, et al. Intestinal alkaline phosphatase targets the gut barrier to prevent aging. *JCI Insight* (2020) 5(6):e134049. doi: 10.1172/jci.insight.134049

22. Looft T, Johnson TA, Allen HK, Bayles DO, Alt DP, Stedtfeld RD, et al. In-feed antibiotic effects on the swine intestinal microbiome. *Proc Natl Acad Sci U.S.A.* (2012) 109:1691–6. doi: doi: 10.1073/pnas.1120238109

23. Okazaki Y, Katayama T. Glucomannan consumption elevates colonic alkaline phosphatase activity by up-regulating the expression of IAP-I, which is associated with increased production of protective factors for gut epithelial homeostasis in high-fat diet-fed rats. *Nutr Res* (2017) 43:43–50. doi: 10.1016/j.nutres.2017.05.012

24. Okazaki Y, Katayama T. Consumption of non-digestible oligosaccharides elevates colonic alkaline phosphatase activity by up-regulating the expression of IAP-I, with increased mucins and microbial fermentation in rats fed a high-fat diet. *Br J Nutr* (2019) 121:146–54. doi: 10.1017/S0007114518003082

25. Shifrin DA, Mcconnell RE, Nambiar R, Higginbotham JN, Coffey RJ, Tyska MJ. Enterocyte microvillus-derived vesicles detoxify bacterial products and regulate epithelial-microbial interactions. *Curr Biol* (2012) 22:627–31. doi: 10.1016/j.cub.2012.02.022

26. Ghosh SS, Gehr TW, Ghosh S. Curcumin and chronic kidney disease (CKD): major mode of action through stimulating endogenous intestinal alkaline phosphatase. *Molecules* (2014) 19:20139–56. doi: 10.3390/molecules191220139

27. Qi M, Liao S, Wang J, Deng Y, Zha A, Shao Y, et al. MyD88 deficiency ameliorates weight loss caused by intestinal oxidative injury in an autophagy-dependent mechanism. *J Cachexia Sarcopenia Muscle* (2022) 13:677–95. doi: 10.1002/jcsm.12858

28. Estaki M, Decoffe D, Gibson DL. Interplay between intestinal alkaline phosphatase, diet, gut microbes and immunity. *World J Gastroenterol* (2014) 20:15650–6. doi: 10.3748/wjg.v20.i42.15650

29. Liu W, Hu D, Huo H, Zhang W, Adiliaghdam F, Morrison S, et al. Intestinal alkaline phosphatase regulates tight junction protein levels. *J Am Coll Surg* (2016) 222:1009–17. doi: 10.1016/j.jamcollsurg.2015.12.006

30. Wu H, Wang Y, Li H, Meng L, Zheng N, Wang J. Protective effect of alkaline phosphatase supplementation on infant health. *Foods* (2022) 11(9):1212. doi: 10.3390/foods11091212

31. Malo J, Alam MJ, Islam S, Mottalib MA, Rocki MMH, Barmon G, et al. Intestinal alkaline phosphatase deficiency increases the risk of diabetes. *BMJ Open Diabetes Res Care* (2022) 10(1):e002643. doi: 10.1136/bmjdrc-2021-002643

32. Yin H-C, Huang J. Effects of soybean meal replacement with fermented alfalfa meal on the growth performance, serum antioxidant functions, digestive enzyme activities, and cecal microflora of geese. *J Integr Agric* (2016) 15:2077–86. doi: 10.1016/S2095-3119(15)61198-4

33. Chilibroste P, Tamminga S, Boer H, Gibb MJ, Den Dikken G. Duration of regrowth of ryegrass (Lolium perenne) effects on grazing behavior, intake, rumen fill, and fermentation of lactating dairy cows. *J Dairy Sci* (2000) 83:984–95. doi: 10.3168/jds.S0022-0302(00)74963-0

34. Zheng M, Mao P, Tian X, Meng L. Effects of grazing mixed-grass pastures on growth performance, immune responses, and intestinal microbiota in free-range Beijing-you chickens. *Poultry Sci* (2021) 100:1049–58. doi: 10.1016/j.psj.2020.11.005

35. Choi KC, Son YO, Hwang JM, Kim BT, Chae M, Lee JC. Antioxidant, anti-inflammatory and anti-septic potential of phenolic acids and flavonoid fractions isolated from lolium multiflorum. *Pharm Biol* (2017) 55:611–9. doi: 10.1080/13880209.2016.1266673

36. Escobar-Correas S, Broadbent JA, Andraszek A, Stockwell S, Howitt CA, Juhász A, et al. Perennial ryegrass contains gluten-like proteins that could contaminate cereal crops. *Front Nutr* (2021) 8:708122. doi: 10.3389/fnut.2021.708122

37. Wati SM, Matsumaru D, Motohashi H. NRF2 pathway activation by KEAP1 inhibition attenuates the manifestation of aging phenotypes in salivary glands. *Redox Biol* (2020) 36:101603. doi: 10.1016/j.redox.2020.101603

38. Cartoni Mancinelli A, Mattioli S, Dal Bosco A, Piottoli L, Ranucci D, Branciari R, et al. Rearing romagnola geese in vineyard: pasture and antioxidant intake, performance, carcass and meat quality. *Ital J Anim Sci* (2019) 18:372–380. doi: 10.1080/1828051X.2018.1530960

39. Wang JP, Hu QC, Yang J, Luoreng ZM, Wang XP, Ma Y, et al. Differential expression profiles of lncRNA following LPS-induced inflammation in bovine mammary epithelial cells. *Front Vet Sci* (2021) 8:758488. doi: 10.3389/fvets.2021.758488

40. Elbing KL, Brent R. Recipes and tools for culture of escherichia coli. *Curr Protoc Mol Biol* (2019) 125:e83. doi: 10.1002/cpmb.83

41. Livak KJ, Schmittgen TD. Analysis of relative gene expression data using real-time quantitative PCR and the 2(-delta delta C(T)) method. *Methods* (2001) 25:402–8. doi: 10.1006/meth.2001.1262

42. Koyama I, Matsunaga T, Harada T, Hokari S, Komoda T. Alkaline phosphatases reduce toxicity of lipopolysaccharides *in vivo* and *in vitro* through dephosphorylation. *Clin Biochem* (2002) 35:455–61. doi: 10.1016/S0009-9120(02)00330-2

43. Campbell EL, Macmanus CF, Kominsky DJ, Keely S, Glover LE, Bowers BE, et al. Resolvin E1-induced intestinal alkaline phosphatase promotes resolution of inflammation through LPS detoxification. *Proc Natl Acad Sci U.S.A.* (2010) 107:14298–303. doi: 10.1073/pnas.0914730107

44. Ichikawa S, Miyake M, Fujii R, Konishi Y. MyD88 associated ROS generation is crucial for lactobacillus induced IL-12 production in macrophage. *PloS One* (2012) 7:e35880. doi: 10.1371/journal.pone.0035880

45. Yasuda T, Takeyama Y, Ueda T, Shinzeki M, Sawa H, Nakajima T, et al. Breakdown of intestinal mucosa *via* accelerated apoptosis increases intestinal permeability in experimental severe acute pancreatitis. *J Surg Res* (2006) 135:18–26. doi: 10.1016/j.jss.2006.02.050

46. Jung Y, Kim H, Min SH, Rhee SG, Jeong W. Dynein light chain LC8 negatively regulates NF-kappaB through the redox-dependent interaction with IkappaBalpha. *J Biol Chem* (2008) 283:23863–71. doi: 10.1074/jbc.M803072200

47. Suzuki T, Yamamoto M. Stress-sensing mechanisms and the physiological roles of the Keap1-Nrf2 system during cellular stress. *J Biol Chem* (2017) 292:16817–24. doi: 10.1074/jbc.R117.800169

48. Hang L, Kumar S, Blum AM, Urban JFJr., Fantini MC, Weinstock JV. Heligmosomoides polygyrus bakeri infection decreases Smad7 expression in intestinal CD4(+) T cells, which allows TGF-β to induce IL-10-Producing regulatory T cells that block colitis. *J Immunol* (2019) 202:2473–81. doi: 10.4049/jimmunol.1801392

49. Liu B, Wang W, Zhu X, Sun X, Xiao J, Li D, et al. Response of gut microbiota to dietary fiber and metabolic interaction with SCFAs in piglets. *Front Microbiol* (2018) 9:2344. doi: 10.3389/fmicb.2018.02344

50. Napier BA, Andres-Terre M, Massis LM, Hryckowian AJ, Higginbottom SK, Cumnock K, et al. Western Diet regulates immune status and the response to LPS-driven sepsis independent of diet-associated microbiome. *Proc Natl Acad Sci U.S.A.* (2019) 116:3688–94. doi: 10.1073/pnas.1814273116

51. Sun X, Cui Y, Su Y, Gao Z, Diao X, Li J, et al. Dietary fiber ameliorates lipopolysaccharide-induced intestinal barrier function damage in piglets by modulation of intestinal microbiome. *mSystems* (2021) 6(2):e01374–20. doi: 10.1128/mSystems.01374-20

52. Mourão JL, Pinheiro VM, Prates J, Bessa RJB, Ferreira LMA, Fontes CMGA, et al. Effect of dietary dehydrated pasture and citrus pulp on the performance and meat quality of broiler chickens. *Poultry Sci* (2008) 87:733–43. doi: 10.3382/ps.2007-00411

53. Ma W, Nguyen LH, Song M, Wang DD, Franzosa EA, Cao Y, et al. Dietary fiber intake, the gut microbiome, and chronic systemic inflammation in a cohort of adult men. *Genome Med* (2021) 13:102. doi: 10.1186/s13073-021-00921-y

54. Schäfer AL, Eichhorst A, Hentze C, Kraemer AN, Amend A, Sprenger DTL, et al. Low dietary fiber intake links development of obesity and lupus pathogenesis. *Front Immunol* (2021) 12:696810. doi: 10.3389/fimmu.2021.696810

55. Cook J, Lehne C, Weiland A, Archid R, Ritze Y, Bauer K, et al. Gut microbiota, probiotics and psychological states and behaviors after bariatric surgery-a systematic review of their interrelation. *Nutrients* (2020) 12(8):2396. doi: 10.3390/nu12082396

56. Ali Q, Ma S, La S, Guo Z, Liu B, Gao Z, et al. Microbial short-chain fatty acids: a bridge between dietary fibers and poultry gut health. *Anim Biosci* (2022) 35 (10):1461–78. doi: 10.5713/ab.21.0562

57. Kaliannan K, Wang B, Li XY, Kim KJ, Kang JX. A host-microbiome interaction mediates the opposing effects of omega-6 and omega-3 fatty acids on metabolic endotoxemia. *Sci Rep* (2015) 5:11276. doi: 10.1038/srep11276

58. Kang C, Zhang Y, Zhu X, Liu K, Wang X, Chen M, et al. Healthy subjects differentially respond to dietary capsaicin correlating with specific gut enterotypes. *J Clin Endocrinol Metab* (2016) 101:4681–9. doi: 10.1210/jc.2016-2786

59. Caesar R, Tremaroli V, Kovatcheva-Datchary P, Cani PD, Bäckhed F. Crosstalk between gut microbiota and dietary lipids aggravates WAT inflammation through TLR signaling. *Cell Metab* (2015) 22:658–68. doi: 10.1016/j.cmet.2015.07.026

60. Suzuki N, Sawada K, Takahashi I, Matsuda M, Fukui S, Tokuyasu H, et al. Association between polyunsaturated fatty acid and reactive oxygen species production of neutrophils in the general population. *Nutrients* (2020) 12 (11):3222. doi: 10.3390/nu12113222

61. Moustafa A. Effect of omega-3 or omega-6 dietary supplementation on testicular steroidogenesis, adipokine network, cytokines, and oxidative stress in adult Male rats. *Oxid Med Cell Longev* (2021) 2021:5570331. doi: 10.1155/2021/5570331

62. Saito Y, Nishio K, Ogawa Y, Kimata J, Kinumi T, Yoshida Y, et al. Turning point in apoptosis/necrosis induced by hydrogen peroxide. *Free Radic Res* (2006) 40:619–30. doi: 10.1080/10715760600632552

63. Dalvi PS, Chalmers JA, Luo V, Han D, Wellhauser L, Liu Y, et al. High fat induces acute and chronic inflammation in the hypothalamus: effect of high-fat diet, palmitate and TNF-α on appetite-regulating NPY neurons. *Int J Obes* (2017) 41:149–58. doi: 10.1038/ijo.2016.183

64. Ishida A, Ohta M, Toda M, Murata T, Usui T, Akita K, et al. Mucin-induced apoptosis of monocyte-derived dendritic cells during maturation. *Proteomics* (2008) 8:3342–9. doi: 10.1002/pmic.200800039

65. Malo MS, Alam SN, Mostafa G, Zeller SJ, Johnson PV, Mohammad N, et al. Intestinal alkaline phosphatase preserves the normal homeostasis of gut microbiota. *Gut* (2010) 59:1476–84. doi: 10.1136/gut.2010.211706

66. Malo MS, Moaven O, Muhammad N, Biswas B, Alam SN, Economopoulos KP, et al. Intestinal alkaline phosphatase promotes gut bacterial growth by reducing the concentration of luminal nucleotide triphosphates. *Am J Physiol Gastrointest Liver Physiol* (2014) 306:G826–838. doi: 10.1152/ajpgi.00357.2013

67. Liu Y, Cavallaro PM, Kim BM, Liu T, Wang H, Kühn F, et al. A role for intestinal alkaline phosphatase in preventing liver fibrosis. *Theranostics* (2021) 11:14–26. doi: 10.7150/thno.48468

68. Ghosh SS, He H, Wang J, Korzun W, Yannie PJ, Ghosh S. Intestine-specific expression of human chimeric intestinal alkaline phosphatase attenuates Western diet-induced barrier dysfunction and glucose intolerance. *Physiol Rep* (2018) 6: e13790. doi: 10.14814/phy2.13790

69. Fukata M, Abreu MT. TLR4 signalling in the intestine in health and disease. *Biochem Soc Trans* (2007) 35:1473–8. doi: 10.1042/BST0351473

70. Santos GM, Ismael S, Morais J, Araújo JR, Faria A, Calhau C, et al. Intestinal alkaline phosphatase: A review of this enzyme role in the intestinal barrier function. *Microorganisms* (2022) 10(4):746. doi: 10.3390/microorganisms10040746

71. Schroeder BO, Birchenough GMH, Ståhlman M, Arike L, Johansson MEV, Hansson GC, et al. Bifidobacteria or fiber protects against diet-induced microbiota-mediated colonic mucus deterioration. *Cell Host Microbe* (2018) 23:27–40.e27. doi: 10.1016/j.chom.2017.11.004

72. Mei AH, Tung K, Han J, Perumal D, Laganà A, Keats J, et al. MAGE-a inhibit apoptosis and promote proliferation in multiple myeloma through regulation of BIM and p21(Cip1). *Oncotarget* (2020) 11:727–39. doi: 10.18632/oncotarget.27488

73. Nakajima S, Kitamura M. Bidirectional regulation of NF-κB by reactive oxygen species: a role of unfolded protein response. *Free Radic Biol Med* (2013) 65:162–74. doi: 10.1016/j.freeradbiomed.2013.06.020

74. Park J, Min JS, Kim B, Chae UB, Yun JW, Choi MS, et al. Mitochondrial ROS govern the LPS-induced pro-inflammatory response in microglia cells by regulating MAPK and NF-κB pathways. *Neurosci Lett* (2015) 584:191–6. doi: 10.1016/j.neulet.2014.10.016

75. Berdyshev AG, Kosiakova H, Nm H. Modulation of LPS-induced ROS production and NF-?B nuclear translocation by n-stearoylethanolamine in macrophages. *Ukrainian Biochem J* (2017) 89:62–9. doi: 10.15407/ubj89.05.062

76. Cario E. Bacterial interactions with cells of the intestinal mucosa: Toll-like receptors and NOD2. *Gut* (2005) 54:1182–93. doi: 10.1136/gut.2004.062794

77. Okorji UP, Velagapudi R, El-Bakoush A, Fiebich BL, Olajide OA. Antimalarial drug artemether inhibits neuroinflammation in BV2 microglia through Nrf2-dependent mechanisms. *Mol Neurobiol* (2016) 53:6426–43. doi: 10.1007/s12035-015-9543-1

78. Ruiz-Núñez B, Pruimboom L, Dijck-Brouwer D, Muskiet F. Lifestyle and nutritional imbalances associated with Western diseases: causes and consequences of chronic systemic low-grade inflammation in an evolutionary context. *J Nutr Biochem* (2013) 24:1183–201. doi: 10.1016/j.jnutbio.2013.02.009

79. Kim K-A, Jeong J-J, Yoo S-Y, Kim D-H. Gut microbiota lipopolysaccharide accelerates inflamm-aging in mice. *BMC Microbiol* (2016) 16:9. doi: 10.1186/s12866-016-0625-7

80. Bates JM, Akerlund J, Mittge E, Guillemin K. Intestinal alkaline phosphatase detoxifies lipopolysaccharide and prevents inflammation in zebrafish in response to the gut microbiota. *Cell Host Microbe* (2007) 2:371–82. doi: 10.1016/j.chom.2007.10.010

81. Morgan MJ, Liu ZG. Crosstalk of reactive oxygen species and NF-κB signaling. *Cell Res* (2011) 21:103–15. doi: 10.1038/cr.2010.178

82. Han H, Zhang J, Chen Y, Shen M, Yan E, Wei C, et al. Dietary taurine supplementation attenuates lipopolysaccharide-induced inflammatory responses and oxidative stress of broiler chickens at an early age. *J Anim Sci* (2020) 98(10): skaa311. doi: 10.1093/jas/skaa311

83. Senger DR, Li D, Jaminet SC, Cao S. Activation of the Nrf2 cell defense pathway by ancient foods: Disease prevention by important molecules and microbes lost from the modern Western diet. *PloS One* (2016) 11:e0148042. doi: 10.1371/journal.pone.0148042

84. Vasconcelos AR, Dos Santos NB, Scavone C, Munhoz CD. Nrf2/ARE pathway modulation by dietary energy regulation in neurological disorders. *Front Pharmacol* (2019) 10:33. doi: 10.3389/fphar.2019.00033

85. Shivakoti R, Biggs ML, Djoussé L, Durda PJ, Kizer JR, Psaty B, et al. Intake and sources of dietary fiber, inflammation, and cardiovascular disease in older US adults. *JAMA Netw Open* (2022) 5:e225012. doi: 10.1001/jamanetworkopen.2022.5012

86. Varadhan R, Yao W, Matteini A, Beamer BA, Xue QL, Yang H, et al. Simple biologically informed inflammatory index of two serum cytokines predicts 10 year all-cause mortality in older adults. *J Gerontol A Biol Sci Med Sci* (2014) 69:165–73. doi: 10.1093/gerona/glt023

87. Kobayashi EH, Suzuki T, Funayama R, Nagashima T, Hayashi M, Sekine H, et al. Nrf2 suppresses macrophage inflammatory response by blocking proinflammatory cytokine transcription. *Nat Commun* (2016) 7:11624. doi: 10.1038/ncomms11624

88. Li Y, Xia D, Chen J, Zhang X, Wang H, Huang L, et al. Dietary fibers with different viscosity regulate lipid metabolism *via* ampk pathway: roles of gut microbiota and short-chain fatty acid. *Poultry Sci* (2022) 101:101742. doi: 10.1016/j.psj.2022.101742

89. Lloyd CM, Snelgrove RJ. Type 2 immunity: Expanding our view. *Sci Immunol* (2018) 3(25):eaat1604. doi: 10.1126/sciimmunol.aat1604

90. Williams JW, Tjota MY, Clay BS, Vander Lugt B, Bandukwala HS, Hrusch CL, et al. Transcription factor IRF4 drives dendritic cells to promote Th2 differentiation. *Nat Commun* (2013) 4:2990. doi: 10.1038/ncomms3990

91. Kole A, Maloy KJ. Control of intestinal inflammation by interleukin-10. *Curr Top Microbiol Immunol* (2014) 380:19–38. doi: 10.1007/978-3-662-43492-5_2

92. Dragović G, Dimitrijević B, Khawla AM, Soldatović I, Andjić M, Jevtović D, et al. Lower levels of IL-4 and IL-10 influence lipodystrophy in HIV/AIDS patients under antiretroviral therapy. *Exp Mol Pathol* (2017) 102:210–4. doi: 10.1016/j.yexmp.2017.02.001